Internal flow variations and diachronous sedimentation within extensive, sustained, density-stratified pyroclastic density currents flowing down gentle slopes, as revealed by the internal architectures of well-exposed ignimbrites on Tenerife

Richard J. Brown[1] and Michael J. Branney[2]

[1]Department of Earth Sciences, Durham University, Durham, DH1 3LE, UK

[2]Geology Department, University of Leicester, University Road, Leicester, LE1 7RH, UK

*Corresponding author: richard.brown3@durham.ac.uk

ABSTRACT

During a protracted explosive eruption, at least four laterally extensive and sustained pyroclastic density currents radiated across the flanks of Las Cañadas volcano, Tenerife. Each pyroclastic current developed marked local and regional spatial variations in response to the incised, gently concave substrate topography. The locations of these variations shifted in space as rapid sedimentation from the current progressively buried and modified the topography. This complex, shifting response of the density currents to minor topographic variations has been reconstructed in high-resolution over a wide area (>500 km^2) using the internal architecture of cryptic time-surfaces ('entrachrons') marked by compositional zoning in the deposit, including variations in clast types. Valley-side field relations reveal that the currents were density-stratified. At a single instant in time, the lower levels of each current comprised a granular-fluid at some locations but were fully dilute and turbulent at others. However, the locations of these variations shifted geographically as the topography changed during the eruption. The variations within the current are recorded by numerous superbly-exposed gradational transitions from various stratified to massive lithofacies, both laterally and in the downcurrent direction. Individual currents were regionally widespread and travelled >15 km, but deposited only in longitudinally-restricted, localised zones that spanned several small valleys and interfluves. The currents bypassed slopes upcurrent and downcurrent of the restricted depositional zones, without depositing. The locations of deposition then gradually shifted with time, such that the extensive deposit sheet was gradually assembled beneath the sustained current in a diachronous fashion. Onlap relationships of internal entrachrons reveal that the base of the ignimbrite sheet and even the bases of individual flow-units are markedly diachronous. Deposition of a flow-unit commenced and ceased at different times in different places. This study suggests that in hazard assessments: (A) models of density currents that incorporate only pre-existing topography (e.g. from DEMs) may give misleading results in the case od sustained currents, because sedimentation from these significantly modifies the topography during emplacement, altering flow paths; (B), frequencies and scales of previous pyroclastic currents determined from pyroclastic successions are likely to be significantly under-estimated because currents commonly bypass without leaving a deposit record; and (C) even where preservation appears to be complete, an ignimbrite at a single exposure commonly will not record the current’s entire flow history at that site.

Keywords: ignimbrite, pyroclastic density current, topography, volcanic hazard, Plinian eruption

Introduction

How density currents interact with substrate topography is of interest to workers on marine turbidite basins, volcanoes, and flood-prone regions (e.g., Fisher 1990, 1995; Valentine et al. 1992; Alexander and Morris 1994; De Rita et al. 1998; Kneller and McCaffrey 1999; Bursik and Woods 2000; Legros and Kelfoun 2000; Kubo 2004; Sulpizio et al. 2008; Doronzo et al. 2010; Gurioli et al. 2010; Lube et al. 2011; Andrews and Manga 2011; Doronzo and Dellino 2012). It is of particular importance to those who work on volcanic hazards at densely populated volcanoes (e.g., Bourdier and Abdurachman 2001; Lirer et al. 2001; Rossano et al. 2004; see also Doronzo and Dellino 2012; Gertisser et al., 2012).

Deposition from particulate gravity currents is fundamentally influenced by substrate topography, and most volcanoes are characterised by substantial relief (e.g., cones, craters and calderas) and many are incised by gullies and valleys. Deposition from density currents typically relates to decelerations resulting from flow divergence (radial flow) or flow down concave slopes (depletive flow; Kneller and Branney 1995; Branney and Kokelaar 2002), including across breaks-in-slope at the base of a volcanic cone, or as a result of encounters with an obstacle in the flow path, as demonstrated in the field, in the laboratory and through modelling (e.g., Valentine, 1987; Macias et al. 1998; Woods et al. 1998; Sulpizio et al. 2007, 2008, 2010; Gurioli et al., 2010; see reviews by Druitt 1998; Branney and Kokelaar 2002; Sulpizio and Dellino 2008). In the past decade, understanding the nature and behaviour of pyroclastic density currents (PDCs) has gained from focus on observed small-volume dome-collapse and Vulcanian eruptions (e.g., Calder et al. 1999; Loughlin et al. 2002; Druitt et al. 2002). Witnessed currents of this type were small-volume, short-lived and depletive, and affected relatively small areas, mostly along valley floors. In contrast, large-volume, radiating PDCs, associated with some large Plinian eruptions, pose a far greater hazard: they are regionally extensive, and they inundate vast areas including over topographic highs within just seconds to hours.

This paper focuses on large-volume radiating density currents, to explore (A) the role of topography, of a range of scales, in influencing deposition from a density current, and (B) how topography changes as a result of deposition by the current. Our analysis draws on an extensive data set of a complex, 3-dimensional internal architecture within a low-aspect ratio ignimbrite sheet, the 273 ka Poris ignimbrite on Tenerife (Edgar et al 2002; Brown et al 2003; Brown and Branney 2004a). This deposit is widespread and was deposited by at least four sustained pyroclastic density currents across irregular topography (Brown and Branney 2004a). The Poris ignimbrite is instructive because it is laterally widespread (500 km^3), compositionally zoned and particularly well-exposed and dissected: these features are not commonly presented together. Detailed logging of 85 vertical sections has enabled us to trace time-surfaces (‘entrachrons’ of Branney and Kokelaar 2002) through the interior of the ignimbrite sheet from valley-to-valley across interfluves and ridges, and also in the downcurrent direction. This has allowed us to reconstruct temporal and spatial variations within the sustained currents on both local and regional scales; how these variations evolved rapidly during the eruption; and how deposition from each density current was highly localised and accompanied by widespread bypassing, resulting in a patchy, incomplete record of the flow history at any individual location. We regard such density current behaviour to typify the behaviour of larger, prolonged density currents on gentle slopes, this increases the potential to underestimate the frequency, duration and dispersal of PDCs in field studies. The study illustrates the importance of meticulous fieldwork in determining the hazards posed by PDC-forming eruptions at large volcanoes. This is of particular importance for volcanoes near the sea because much of the depositional mass transported by PDCs may end-up concealed offshore**.**

The sedimentation of ignimbrite

The depositional mechanisms of catastrophic currents that produce large ignimbrites are thought to be gradational between fluid-modified granular flows and particle-bearing fluids (Branney and Kokelaar 2002). Such gradational currents are poorly understood. Direct observation of their deposition is impossible, not least because they are capricious, opaque and hazardous. Over the past three decades studies on the architecture of large ignimbrite sheets (e.g., Taupo ignimbrite, New Zealand, Wilson and Walker 1985; Valley of Ten Thousand Smokes ignimbrite, Alaska, Fierstein and Hildreth 1992; Fierstein and Wilson 2005; 1991 eruption of Pinatubo, Philippines, Scott et al. 1996; Branney and Kokelaar 2002; Zaragoza ignimbrite, Mexico, Carrasco-Nüñez and Branney 2005) have provided insights into the depositional mechanisms of PDCs. Our understanding of the transport and deposition of ignimbrite derives largely from inferences from such deposits, from laboratory experiments (e.g. Choux and Druitt, 2002; Roche et al. 2005, 2011; Girolami et al. 2010; Roche 2012) and the numerical modelling of selected physical parameters (e.g. Valentine 1987; Dade and Huppert 1996; Woods et al 1998; Druitt 1998; Denlinger and Iverson 2001; Burgisser and Bergantz 2002; Dufek et al., 2009; Doronzo et al. 2010; Andrews and Manga 2012). However, models and experiments are not yet sufficiently sophisticated to account for the range of common ignimbrite lithofacies, nor their complex architectures.

Large-volume ignimbrites derive from protracted currents that may last for minutes to hours (e.g., 1991 eruption of Pinatubo, Philippines, Scott et al. 1996). The deposits of sustained particulate density currents can be complex, and exhibit rapid vertical and lateral lithofacies transitions (e.g. Scott et al. 1996; Bryan et al. 1998b; Allen and Cas 1998; Brown and Branney 2004a, 2004b; Pittari et al. 2006). This complexity has led workers to consider that sustained currents are inhomogeneous in both space and time, i.e., their velocity, concentration, capacity and rheology can change spatially and temporally during transport and deposition (e.g., Branney and Kokelaar 1992, 2002; Kneller and McCaffrey 1991; Best et al. 2005; Andrews and Manga 2012). In such currents a range of different clast-support mechanisms operate in tandem during transport and deposition (Branney and Kokelaar 2002), so that adjacent clasts within the resulting ignimbrite may have had different transport histories. Flow directions of sustained density currents also vary with time at individual locations (Kneller et al. 1999; Morris and Alexander 2003; Branney et al. 2004; Andrews and Branney 2012).

The depositional mechanisms of sustained PDCs are fundamentally influenced by lower flow-boundary conditions, which as the result of density stratification in the current will differ significantly from conditions higher in the current (Fisher 1966; Valentine 1987; Branney and Kokelaar 1992, 1997, 2002; Sohn 1997; Sulpizio et al. 2007; Sulpizio and Dellino, 2008). The flow-boundary zone includes the basal part of the current and the uppermost part of the deposit, and it rises as the deposit aggrades. Over the past decade researchers have recognised a continuum of flow-boundary zone conditions that give rise to a range of PDC deposit types as a function of current velocity, shear rate, and particle concentration in the lower parts of the current, and sedimentation rate (e.g., Branney and Kokelaar 2002; Burgisser and Bergantz 2002; Sulpizio et al. 2007).

Branney and Kokelaar (2002) proposed that four intergradational end-member types of flow-boundary (direct-fallout-dominated, traction-dominated, granular flow-dominated and fluid-escape-dominated) account for the range of common lithofacies in ignimbrites. Each end-member type of flow-boundary zone is characterised by distinctive velocity and concentration gradients, yet they are considered transitional into one another with changing rates of concentration, deposition and shear. The vertical succession of lithofacies within the deposit of a sustained current records the changing conditions and depositional processes with time (unsteadiness), while the lateral lithofacies variations along an entrachron record spatial variations during a single moment in time (non-uniformity, see Kneller and McCaffrey 1999; Choux and Druitt 2002; Branney and Kokelaar 2002).

Eruptive history and morphology of Las Cañadas volcano

Tenerife is composed of a large ignimbrite shield volcano, Las Cañadas volcano, constructed on coalesced and eroded basaltic shield volcanoes (Ancochea et al. 1990; 1999; Martí et al. 1994; Fig. 1). Numerous Plinian eruptions have occured in the past 2 Ma (Ancochea et al. 1990; Huertas et al. 2002; Brown et al. 2003; Dávila Harris, 2009; Dávila Harris et al. 2011). These deposited ignimbrites, and pumice and ash fall deposits across the island. The pyroclastic deposits are interleaved with numerous basaltic lavas from scattered monogenetic flank volcanoes, and from three volcanic rift-zones (Bryan et al. 1998a, b; Bryan et al. 2000; Pittari et al., 2006; Dávila Harris 2009; Dávila Harris et al. 2012). The southern flank of Las Cañadas volcano rises to 2.5 km above sea-level and drops abruptly back down to 0.5 km into the central caldera (Figs 1 and 2). For the purposes of this paper we consider that the southern flanks include a 180° sector that stretches from the north side of the Güimar valley to Guia de Isora in the west (Fig. 2). This southern flank is broadly concave, from steeper upper flanks (9–15°; Fig. 2) to lower gradient (<6°) coastal flanks (<200 m altitude; the Bandas del Sur) that reach as much as 5 km inland from the coast. The flank varies from 15–20 km wide. In detail, the lower gradient apron is not continuous and forms a coastal crescent that stretches from Los Cristianos in the west to just north of Poris de Abona. The eastern end of the southern flank of Tenerife is abruptly terminated by the partly filled Güimar collapse scarp, which is the result of one of several large sector-collapse landslides that have occurred on Tenerife over the past 2 Ma (Watts and Masson 2001; Dávila Harris et al. 2011).

The Bandas del Sur has a semi-arid climate prone to periodic flash floods, which have incised the slopes to produce a network of downhill-converging radial valleys. Palaeotopography indicates that the region has had a similar topography for the past 2 Ma (Pittari et al. 2006). Valleys and palaeo-valleys are 10–50 m deep, 10's to 100's of metres wide, and are separated by hundreds of metres-wide, flat-topped interfluves and narrower ridges (Fig. 1).

Terminology

We use pyroclastic density current (PDC) for any type of gaseous gravity current carrying pyroclastic material (i.e. including both 'fully-dilute' and 'granular fluid-based' types; Branney and Kokelaar 2002), and we use ignimbrite for the pumiceous deposit of a PDC (including ash-rich deposits). The term ignimbrite sheet is used to describe a succession of ignimbrites and subordinate fall deposits deposited during one eruption. We use the term valley-fill to describe those parts of the ignimbrite sheet deposited within valleys and the term veneer in a non-genetic sense, to describe topography-draping, thinner ignimbrite deposited on topographic highs (similar to 'overbank facies' of Schumacher and Schmincke 1990): no inference of deposition from the 'tail' of a PDC is implied (cf. IVDs of Walker et al. 1981). The term flow-unit is used to define an ignimbrite bounded by horizons (such as fall deposits, reworking, scours) that indicate pauses in current activity at that site. Lithofacies are summarised in Brown and Branney (2004a). We use the term entrachron to describe a cryptic surface within an ignimbrite that links together clasts that entered the current at the same time (e.g., a new type of juvenile material) and depochron to describe a cryptic surface that links together clasts that were deposited at the same time. We use the lithostratigraphic term 'member' for a lithologically-distinctive division that has regional distribution (see Brown and Branney 2004a): members do not necessarily correspond to individual flow-units.

Ignimbrite architecture of the Poris Formation

The 273 ka Poris Formation (Bryan et al. 1998a; Egdar et al. 2002; Brown et al. 2003; Brown and Branney 2004a) lies within the Quaternary Bandas del Sur Group of Tenerife (Fig. 2). It is a compound phonolite to tephri-phonolite ignimbrite sheet, composed of several ignimbrite flow-units with associated co-ignimbrite ash fall layers and pumice fall deposits emplaced during a Plinian eruption (Fig. 3). It outcrops in the Diego Hernandez sector of Las Cañadas' caldera wall (Edgar et al. 2002; Smith 2012) and along the southeast coast (Fig. 4; Bryan et al. 1998a; Edgar et al. 2002; Brown et al. 2004a). Proximal sections of the ignimbrite sheet are interpreted in Smith (2012). The present study focuses on the coastal ignimbrite sheet, which is widely 2–35 m thick and emplaced across a gently concave volcano flank cut by small dendritic valleys (10–40 m deep), separated by broad interfluves, which it variously draped and buried along a 50 km-long coastal strip (from Montaña Guaza near Los Christianos in the south, to El Baul in the northeast, Fig. 1).

The Poris Formation has been subdivided into eleven lithostratigraphic members and includes four ignimbrite flow-units (Fig. 3; Brown and Branney 2004a). Each of the four flow-units is separated by clear evidence for pauses in density current activity (e.g., pumice or ash fall layers, or eroded remnants of these). Flow-units 1–3 are composed mostly of massive lapilli-tuff within palaeovalleys and extensive ash layers across palaeo-ridges (Fig. 3). Flow-unit 4 is zoned, allowing it to be divided into four distinct lithostratigraphic members, and can be traced across the entire width of the Bandas del Sur (Fig. 4). Its compositional zoning has the form of compositional variations with height in the deposit, in the form of cryptic entrachrons that mark the entrances and exits of various distinctive components, including accretionary lapilli, abundant lithic clasts, and juvenile banded tephri-phonolite pumice clasts. However, there is no evidence within the flow-unit for the cessation of flow (i.e., no ash fall layers or reworking; see Brown and Branney 2004a). Moulds of allochthonous tree trunks are common in Flow-unit 4.

Distribution of ignimbrite flow-units of the Poris Formation

The distribution of each flow-unit varies considerably (Fig. 4). Flow-units 1 and 2 are restricted to a 10–20 km-wide zone in central parts of the Bandas del Sur (mostly between Tajao and Poris de Abona, Figs. 1 and 4). As they were the first ignimbrites to be emplaced they were thickest along valley axes, but the thickest valley fills have been eroded and the ignimbrites are preserved mostly as remnants along palaeo-valley sides and as centimetre-thick veneers over palaeo-ridges. The maximum preserved thicknesses are 2.6 m (Flow-unit 1 at Montaña Magua) and 2.2 m (Flow-unit 2). Flow-unit 3 outcrops between La Caleta and Montaña Magua (Fig. 1) and is preserved up to 93 cm thick in palaeo-valleys (between Tajao and La Caleta, Fig. 4).

Flow-unit 4 is much more extensive and overlaps all underlying flow-units (Fig. 4). Its outcrop width exceeds 37 km (between Aldea Blanca and Güimar; Figs 1 and 4). Internal entrachrons (marked by appearances and disappearances variously of accretionary lapilli, abundant lithic clasts, and tephri-phonolite pumice) reveal that the distribution of the current gradually increased with time (Fig. 4), and that later parts of the current (Member 9) entered the Güimar valley for the first time during the eruption. The flow-unit is thickest (>35 m) and most complete in central parts of the Bandas del Sur (e.g., La Caleta to Fasnia; Fig. 1). In the west it is generally thinner (<10 m) and only comprises later parts of Flow-unit 4 (Members 6–9) overlying Member 1 pumice and ashfall layers. In the East (Güimar valley, Fig 1) the ignimbrite sheet comprises only the latest parts (Member 9), locally with ashfall and pumice fall layers (Fig. 4). Ignimbrite is absent where the coastal flanks are steeper (between Fasnia and Güimar; Fig. 3).

Each ignimbrite flow-unit has an associated thin (cm-thick) co-ignimbrite ash fall layer. These ash layers are predominantly composed of ash pellets. They are more extensive than the ignimbrites, and covered much of the south coast of Tenerife (see Brown and Branney 2004a; Brown et al. 2010).

Longitudinal (parallel-to-current) architecture

The Poris ignimbrite sheet is absent on the steeper (9–15°) upper flanks of Cañadas volcano, but is present locally in the caldera wall and on the nearby upper NE flank (Edgar et al. 2002; Smith 2012). More generally, the ignimbrites are preserved on the less steep (<4°) slopes of the coastal pyroclastic apron (Fig. 3) within 5 km of the present coastline, but rarely above ~200 m altitude. The general absence of ignimbrite on the steeper (>4 °) slopes cannot be an artefact of subsequent erosion because (1) the enclosing fall deposits extend upslope beyond where the ignimbrites of the lower slopes pinch out; and (2) the architecture of the ignimbrite sheet shows that the original proximal edge of the ignimbrite is preserved on the lower gradient slopes (Fig. 5). The upper surfaces of the ignimbrite sheet generally dip 1–4° seaward, and the sheet pinches out up the broadly concave slope at 300–400 m altitude (Fig. 5).

The coastal apron provides excellent continuous 5 km-long longitudinal sections through the Poris ignimbrite sheet. Tracing the individual ignimbrite flow-units and the entrachrons within them in a downcurrent direction (see Fig. 5) has enabled the internal architecture to be reconstructed in a parallel-to-current orientation. This architecture is well illustrated in a ~1 km-long continuous section north-west of Montaña Magua (Fig. 5) where three ignimbrite flow-units (1, 2 and 4) are preserved in a current-parallel section both along a fossil interfluve and along a palaeo-valley. Both along the interfluve and along the valley axis, successive flow-units onlap in the upcurrent direction against the regional slope (Fig. 5): Flow-unit 1 thins upslope from 2 m to <0.06 m over a distance of ~100 m; Flow-unit 2 thins from 15 m to 2 m over the same distance (Fig. 5). Upslope, these flow-units pass into thin ash veneers that are texturally indistinguishable from the veneer deposits that they grade into laterally across palaeo-ridges (Fig. 5).

Flow-unit 4 also onlaps against the slope and thins from ~35 m (reconstructed thickness, Fig. 5) to 0 m upslope over a distance of <900 m. Entrachrons within it pick out similar internal retrogradational relationships with topography (Members 6-9 on Figs 5 and 6A-C). This onlapping, retrogradational architecture is repeated on a smaller scale producing a giant bedform in Flow-unit 4 at

Montaña Magua (Brown and Branney 2004b). Thus, the retrogradational geometry of the flow-units and their internal architectures mirrors the geometry of the entire ignimbrite sheet (Fig. 6D). The proximal edge of the ignimbrite sheet and all units within it have a 'feather edge' geometry (Fig. 6D; also exposed in quarry faces at El Arrecife). Similar onlapping retrogradational architectures are also seen in the Abades ignimbrite (Fig. 7F).

Tranverse (sideways-to-current) architecture: gradations from valley-fill to veneer facies

Lateral variations from thin veneers of ignimbrite on palaeo-ridges to thicker valley-fill ignimbrite in palaeo-valleys are well preserved. Several near-complete valley cross-sections are exposed at Montaña Magua, and we focus on these (Figs 1 and 7).

Flow-units 1 and 2

Near Montaña Magua the lower two flow-units each comprise an ignimbrite overlain by an extensive ash pellet fall layer (Figs. 3 and 7). Flow-unit 1 comprises up to 2.5 m thick, ash-rich yellowish lapilli-tuff with scattered accretionary lapilli. Flow-unit 2 comprises up to 15 m of poorly sorted massive lapilli-tuff, with local clast-supported pumice lenses along the palaeovalley sides. The ignimbrites are thickest in palaeovalleys, where they are lenticular in cross-section and flat topped (Fig. 7A-C). Moulds of small shrubs and current-orientated delicate twigs and grasses are commonly preserved along their bases. Complete gradations from valley-fill to veneer facies are exposed for flow-units 1 and 2 (Fig. 7). The ignimbrite veneers are laterally extensive across palaeo-ridges and are found on slopes as steep as 35°. They are typically several centimetres thick and are composed of massive tuff. Diffuse stratification is present at some localities. They locally thicken into shallow topographic depressions. The upper parts of both the valley-fill and veneer ignimbrites contain scattered accretionary lapilli and each ignimbrite flow-unit is overlain by an extensive, thin co-ignimbrite ash fall layer made of ash pellets (Brown and Branney 2004a; Brown et al. 2010; ash pellets are AP1 type of Brown et al. 2012).

Flow-unit 4

The lowermost part (Member 6) of Flow-unit 4 is geographically restricted with abundant large accretionary lapilli (Fig. 7). Within palaeovalleys it reaches 12 m thick and is massive. Diffuse bedding gradually appears within upper parts and towards palaeovalley margins, where initially indistinct, bedding gradually becomes more distinct and also more close-spaced, so that the massive valley-fill ignimbrite grades imperceptibly into the thinner, diffuse-stratified veneer facies (Fig. 7; this is 'splay-and-fade' stratification of Branney and Kokelaar 2002). The veneer component of Member 6 is complex with rapid lateral variations. It typically comprises a decimetre-thick unit of diffuse-bedded to stratified tuff and accretionary lapilli-rich lapilli-tuff with scattered pumice and lithic lapilli (see Brown et al. 2010; Fig. 7). Discontinuous planar scour surfaces separate beds, which lack accretionary lapilli in their lower portions. Low-angle cross-stratified tuff occurs locally at the base of these beds. Accretionary lapilli (AP2 types of Brown et al., 2012) are 10 times as abundant in the thin topography-draping veneer ignimbrite (~400–500/m^2) as they are in the coeval thicker, valley-filling ignimbrite (≤50/m^2). Elsewhere around Montaña Magua, the veneer ignimbrite exhibits stratification defined by discontinuous lenses and layers of lithic lapilli, pumice lapilli or accretionary lapilli. Small steep-sided scours are also present (see Brown and Branney 2004a).

Within Flow-unit 4, Member 6 passes up into Member 7 ignimbrite that lacks accretionary lapilli (Figs. 2 and 7). Within the palaeovalleys, Member 7 is >20 m-thick, homogenous massive lapilli-tuff. Laterally, this passes gradationally across palaeovalley sides into an extensive veneer ignimbrite, typically 2–5 m thick (Fig. 7). Within the veneer of Flow-unit 4, the contact between members 6 and 7 is sharp and marked by a scour surface. At many localities within the veneer, Member 7 includes stratified, cross-stratified, diffuse-bedded and massive lapilli-tuff. Subtle, complex vertical grading patterns (normal and inverse) of lithic and pumice lapilli are common. Individual beds and strata are discontinuous over metres to decimetres and it is not possible to trace them between outcrops. Pods, lenses and thin layers of clast-supported pumice or lithic lapilli and blocks are common throughout the veneer facies; in places they exhibit load-and-flame structures, some of which are sheared in a downslope direction. Shallow to steep-sided and poly-phase scours and diffuse low-angle truncations that pass laterally into diffuse-bedding and then fade out laterally into massive lapilli-tuff are common (‘scour splay-and-fade stratification’ of Branney and Kokelaar 2002). A 9 m long by 0.4 m high dune bedform outcrops at Montaña Magua and was described in detail by Brown and Branney (2004b).

Member 7 passes up abruptly into Member 8, a widespread coarse-grained, clast-supported lithic-rich grey to pink ignimbrite that reaches 15 m-thick within palaeovalleys (Fig. 7). To the north of Montaña Magua it typically has a preserved thickness of 2–3 m and passes laterally into a 0.3–1 m-thick topography-draping veneer. It lacks the abundant lithic lapilli, blocks and boulders seen elsewhere in this member (see Brown and Branney 2004a). The juvenile pumice changes from highly vesicular phonolite to dense and variably vesicular, banded tephri-phonolite (Brown and Branney 2004a). The first appearance of the more mafic juvenile material can be traced throughout the ignimbrite sheet as an entrachron, as can the base of the lithic breccia, marked by the first appearance of abundant quantities of lithic clasts within the flow-unit. Metre-scale scouring of the underlying units has occurred locally (e.g. at Tajao, Fig. 1), but elsewhere the base exhibits spectacular load structures and pods into the underlying Member 7 ignimbrite. Member 8 passes gradationally upwards into Member 9 which is only preserved as a veneer facies pumiceous lapilli-tuff <1 m thick. It is commonly composed of clast-supported pumice lapilli and blocks. Its across-valley geometry and lithofacies transitions are not well constrained.

In summary, the ignimbrite flow-units are thick in palaeovalleys and thin over palaeo-ridges (Fig. 7D). The early flow units (1–3) thin markedly over palaeo-ridges, with thickness ratios of the order of 100:1. In contrast, the difference in thickness between coeval ignimbrite in palaeovalleys and palaeoridges in Flow-unit 4 is much less (<5:1; see Fig. 7D).

Interactions between density currents and topographic obstacles

Basaltic scoria cones up to 300 m high pepper the lower flanks of Las Cañadas volcano (see Bryan et al. 1998a; Kröchert and Buchner 2009; Fig. 8A). During explosive eruptions they obstructed PDCs and resulted in the upstream accumulation of anomalously thick sequences of ignimbrite. An instructive example of this can be seen in the Güimar valley (Fig. 1) — an 8 km wide, flat-bottomed scarp formed by catastrophic sector collapse of the SE flank of Tenerife. The Poris density currents flowed down the Guimar valley, and across two close-spaced scoria cones situated 1.5 km from the present coastline (Fig. 9). Long axes of imbricated tree moulds are aligned parallel to flow direction (towards the SE) and indicate that the current passed over the scoria cones (Fig. 9). However, Flow-unit 4 is anomalously thick between and upstream of the scoria cones: it is predominantly massive and exceeds 13 m in thickness immediately upstream of the northernmost scoria cone (Flow-unit 4, Fig. 9). It then thins to 3–6 m over the upstream sides of the scoria cones (logs B and D on Fig. 9). Yet, on flat ground downstream and laterally away from the cones, the density current apparently did not deposit anything, because the ignimbrite flow unit is absent there and the Poris Formation comprises only the ash fall and pumice fall layers (logs A and E on Fig. 9).

Another example of enhanced deposition of ignimbrite upstream of a cone is seen at the ~100 m-high Fasnia scoria cone (Fig. 8A). Here, massive ignimbrites of the Fasnia Formation exceed 7 m thick on the stoss side of the cone (Fig. 8B) while on the lee side the same ignimbrites are only a few centimetres thick and stratified, and they laterally pass into low-amplitude scour surfaces that cut the through underlying pumice fall deposits.

Discussion

Topography affected the extensive, radiating pyroclastic density currents (PDCs) on various different scales. These are discussed below.

Controls on the distribution of pyroclastic density currents

Differences between the distributions of the four ignimbrite flow-units (Fig. 4) are attributed to a combination of: (1) changing eruption dynamics; and (2) simultaneous depositional modification of the topography by the density currents. Although comparison of volume of each flow-unit is precluded by flow into the sea, the field relations strongly suggest that the volumes of the first three density currents were lower than those of the fourth current, resulting in Flow-units 1–3 having narrower geographic distributions. In addition, in-situ shrub moulds along the bases of Flow-units 1–3 indicate that these early currents had lower velocities, in contrast to the larger current that deposited Flow-unit 4, which was not only more laterally extensive and capable of transporting lithic blocks 15–20 km from source, but it also stripped mature forest from upper slopes, leaving widely scattered (allochthonous) tree moulds on the coastal plain. As the Poris eruption progressed, the valley/interfluve topography on the lower coastal flanks of Tenerife was gradually infilled by ignimbrite and, as a result, the later currents were less valley-confined (Figs. 5–7). We infer that this was the result of increasing overspill of small-volume PDCs from one valley into adjacent valleys.

During deposition of Flow-unit 4 the rapid increase in the geographic footprint of the density current (Fig. 4) in inferred to have resulted from increases in the mass-flux of the eruption (waxing flow) with a consequent increase in the volume of the density current. The rapid and marked lateral advance of the PDC across the region in eastwards and westwards directions, perpendicular to the flow-direction during the deposition of Flow-unit 4 (Fig. 4) also likely resulted from an increase in the volume of the density current during the climactic stages of the eruption. The current increased not only in capacity (the bulk mass of material carried) and spread out more, but its competence also increased, as recorded by the presence of abundant large lithic blocks and boulders in Member 8. Waxing flow, recorded by the upwards-coarsening, seems to have favoured widespread erosion and entrainment as recorded by the allochthonous tree trunks, lenses of locally-derived lithic clasts, and the presence of metre-scale scour surfaces in the deposits in Flow-unit 4 (Brown and Branney 2004a). Proximally, the increased eruptive mass-flux may also have favoured the current overtopping a broader stretch of the Las Cañadas caldera rim (Fig. 1).

Influence of regional-scale topography on deposition from PDCs

On a regional scale, deposition from the Poris density currents was strongly controlled by the large-scale morphology of the ignimbrite shield volcano. Geographic zones of contrasting PDC behaviour can be delineated along the southern flanks of Cañadas volcano (Fig. 10). Deposits in the most proximal regions (i.e., intra-caldera 1–5 km from source) are not available for study, but comparison with ancient dissected calderas suggests that thick accumulations of ignimbrite and lithic breccia were deposited from PDCs that were partially contained within caldera walls (e.g., the Ordovician Scafell Caldera, Lake District, Branney and Kokelaar 1994). Proximal parts of the ignimbrite sheet (<5 km from source) are preserved in the present caldera wall and reach 30 m thick, and are considered to have accumulated in a broad valley oriented east-west away from the caldera walls (Smith 2012).

In medial zones (>5–15 km from source, Fig. 10) the PCDs flowed away from the caldera down the steep upper flanks of Las Cañadas volcano. We infer from the absence of ignimbrite in these regions that the PDCs bypassed these steep slopes with accumulative to near-uniform flow capacity (e.g., Kneller and Branney 1995) and remained largely non-depositional for most of their passage to the sea.

In distal regions (>15 km from source; Fig. 10) the PDCs started to deposit, presumably caused by passage onto the more gentle (<6°) coastal slopes. We infer that the density currents deposited there as a result of depletive flow capacity (e.g., Kneller and Branney 1995); that is, the spatial decelerations incurred by flow across the regional concave slope. This, combined with the depletive effect of slightly divergent (radiating) flow paths around the island reduced the current’s capacity to transport its particulate load, promoting deposition as the current encountered gradually less-steep slopes with proximity to the coast (Fig. 1). Similar processes have been demonstrated in laboratory experiments of aqueous density currents (Garcia and Parker 1989; Mulder and Alexander 2001; Kubo 2004), in numerical simulations (Kassem and Imran 2001) and, for example, where PDCs elsewhere crossed breaks-in-slope (e.g., Roobol et al. 1987; Giordano 1998; Macías et al. 1998; Sulpizio et al., 2007, 2010; Sulpizio and Dellino 2008). It is possible that the reduced gradient of the more coastal parts of the pyroclastic apron may have forced the current to undergo a downstream transition from supercritical to subcritical flow (e.g., hydraulic jump; Van Andel and Komar 1969), but this is not a requirement for deposition and is difficult to established from deposits (e.g. Gray et al. 2005). Turbulence can be generated at a hydraulic jump and this may promote substrate erosion and entrainment, and enhanced mixing with the ambient fluid (e.g., Komar 1971).

We note that scours of all scales occur within Flow-unit 4 deposits in areas where there is evidence for bypassing (i.e., the proximal edge of the coastal ignimbrite sheet, see Brown and Branney 2004a). This indicates that at these areas, substantive accelerations were close to neutral (bypassing with neither overall deposition nor erosion; Branney and Kokelaar 2002) such that relative minor fluctuations in the current (such as pulses or passage of eddies or roll waves) would have been sufficient to induce minor, ephemeral erosion and deposition.

The gradient between the caldera and the coast varies around the volcano. For example, locally on the SE flank, and widely around the north flank, the low-gradient coastal apron is absent, with steep slopes extending all the way to the sea (Figs. 1 and 2). Some of the shortest (14 km) and steepest (consistently >9^{o}) flanks on the southern side of the island occur between Fasnia and Güimar (Fig. 2). Poris ignimbrites are widely absent in this section, even at the coast. In this sector of Tenerife, the Poris PDCs bypassed all the way to the sea. We can deduce this because the fall deposits are present in the area and Poris ignimbrite is preserved proximally, directly upslope of this region in the Diego Hernandez caldera wall (Edgar et al. 2002; Smith 2012). We infer that the steeper coastal slopes in this region ensured that capacity of the PDCs remained uniform or accumulative and non-depositional all the way to the sea so that left little or no record was left of their passage.

The bypassing behaviour of the Poris PDCs across the flanks of Tenerife indicates that they were autosuspending currents in a near-equilibrium state (neither eroding nor depositing), similar to the behaviour of some turbidity currents in submarine channels (Stevenson et al. 2012). This condition exists where substantial accelerations approximate to zero (fig 1.1 of Branney and Kokelaar 2002), and this, in turn, depends upon the interplay between any changes in mass flux at source (e.g. eruption dynamics) and the particular configuration of the substrate slope. With a steady input at source, spatial changes in slope induce spatial accelerations (accumulative flow) or decelerations (depletive flow) and thus exert a primary control on the current dynamics and on whether the current erodes, bypasses or deposits (e.g., Kneller and Branney 1995; Mulder and Alexander 2001; Brown and Branney 2004b; refs in Sulpizio and Dellino 2008). The gentle slopes of the coastal pyroclastic apron on Tenerife are composed of ignimbrite sheets, and is similar to turbidite fan systems constructed at the mouths of submarine channels. Proximal scour-and-fill basin-facies turbidites deposited near the start of more gentle slopes are inferred to result from currents that alternated between erosion and deposition (e.g., Kokelaar 1992; Amy et al. 2007) and are, we suggest, analogous to the proximal feather-edge of the coastal Poris ignimbrite sheet.

Other ignimbrites in southern Tenerife show similar distributions, thinning and then pinching out up the concave flank, and we suspect that all PDCs on Tenerife behaved in a similar manner to those of the Poris eruption. Given that the Poris PDCs were depositing thick ignimbrite in proximal extracaldera regions, and that runout distance is closely linked to sedimentation (Andrews and Manga 2012), we infer that passage down the long and steep slopes inhibited sedimentation in medial reaches and increased the runout distances and the ignimbrite mass-loading on the coastal apron and offshore.

The internal onlapping architecture of the Poris ignimbrite sheet (Fig. 6D) means that the bases of the flow-units, and also the base of the ignimbrite sheet as a whole (excluding the fall layers) are diachronous. Each current did not commence deposition at the same time at all localities across the region. Rather, the onset of deposition migrated upcurrent with time during passage of the current and this advance continued until it reached what is now the proximal ‘feather-edge’ of each ignimbrite flow-unit (Fig. 6D). This is particularly well illustrated by Flow-unit 4, which was deposited from a sustained current that experienced several marked changes in the composition of clasts supplied to it through time (e.g., Fig. 5). Entrachrons that enclose compositionally diverse units onlap against the topography.

The complex onlap architecture is illustrated in more detail by the giant regressive bedform in Member 8 (see Brown and Branney 2004b). It resulted from a sustained PDC that was just entering into a region of deposition at that location. The diachronous character of the Poris ignimbrite sheet means that individual vertical sections through the ignimbrite do not record the entire depositional history of the parent PDC—the same holds true for each individual flow-unit. In general, the onlap relationships suggest that a large proportion of the pyroclastic load of the PDCs was deposited at sea: there is a substantial thickness of pyroclastic material offshore southern Tenerife (Bogaard 1998).

The architectural relationships in the Poris ignimbrite sheet resulted from unsteadiness and non-uniformity in sustained density-stratified PDCs, and they are picked out by entrachrons. However, in massive, homogenous ignimbrite sheets, such as are generated during super-eruptions, these relationships may go unrecorded and the changing position of the aggradation surface during the eruption will remain cryptic. Defining and tracing entrachrons in apparently homogeneous large-volume (100–1000 km^3), ignimbrite sheets would be useful in understanding their emplacement history, and may provide clues about the durations of sustained PDCs during cataclysmic eruptions. Analysis of smaller-volume zoned ignimbrite sheets with well defined architectures, such as the Poris ignimbrite, can provide critical clues to help in this endeavour.

The interaction of PDCs with local topography

The valley-fill to veneer lithofacies transitions in the Poris Formation ignimbrite flow-units (Fig. 7) record changes in flow-boundary conditions laterally across topography, i.e., flow-boundary non-uniformity. These differences are primarily the result of a density-stratified current interacting with irregular topography (e.g., Valentine 1987; Pittari et al. 2006). Different topographic elevations project into different levels within the current that have differing particle concentrations, turbulence intensities, compositions (e.g., proportions of ash vs. pumice lapilli) and clast-support mechanisms. Thus, the character of the lower flow-boundary zone that developed within the base of the current vary with elevation.

In the lower flow-units (1–3), lateral transitions from thick massive lapilli-tuff (valley-fill facies) to thin tuff (veneer facies; Fig. 7) record deposition from strongly density-stratified pyroclastic currents that transported the majority of their coarse lapilli along valley axes. The thin ignimbrite veneers lack abundant pumice lapilli and indicate that higher levels (metres to tens-of-metres above the base) within the density-stratified current inundated the local topographic highs, but carried predominantly fine ash.

The marked veneer-to-valley-fill transitions in flow-units 1–3, are similar to those documented in the Oruanui ignimbrite, New Zealand (type B deposits of Wilson 2001). The thinness of the Oruanui veneer deposits was attributed to the 'fluidity' of the PDCs, helped by the presence of water in the substrate on the palaeo-valley walls (a 'hot-skillet' analogy), which is inferred to have promoted the downhill movement of coarse lapilli. However, coarse lapilli are absent in the Poris Formation on the wide, plateau-like interfluves, which suggests that the extensive upper levels of the Poris PDCs that travelled across the broad interfluves transported few coarse lapilli, in contrast to the current's lower, more concentrated levels that were more channelised along the valleys and evidently contained abundant coarse pumice. Steam-flashing of water in the substrate (Wilson 2001) would widely disrupt bedding, and is not recorded in the basal pumice fall layers of the Poris Formation. Moreover, the nature of the palaeosol and the spacing of in situ fossil shrubs indicate that the Poris deposits were emplaced in a dry desert landscape similar to that of the present day southern coast. The architectural relationships across palaeo-valleys (e.g. near Montaña Magua; Fig 1) allow some constraints to be placed on the thickness of the lowermost, more concentrated pumice lapilli-bearing levels of the currents at valley axes (Fig. 7). The lower, concentrated levels cannot have been thicker than the current depth of palaeovalleys or pumice and lithic lapilli would have been deposited widely upon the interfluves. We thus infer that lower, concentrated and lapilli-bearing levels of most of the density stratified current were probably less than several metres thick.

Insights into flow non-uniformity over topography can be gleaned by using the height in the deposit at which accretionary lapilli appear and disappear as time-lines. Evidence from numerous ignimbrite sheets on Tenerife indicated that accretionary lapilli initially nucleated in the form of small ash pellets within the buoyant atmospheric co-ignimbrite ash plumes (Brown et al. 2010). These pellets fell out into the current over both valleys and topographic highs and were eventually deposited within the ignimbrite. Additional layers of fine ash accreted to the pellets during their passage through the co-ignimbrite-density current system transforming the ash pellets into accretionary lapilli (Brown et al. 2010; also see Van Eaton and Wilson 2012). It is known that they fell directly into the lower parts of the Flow-unit 4 current rather than having been carried from proximal locations by the current because, pumice lapilli and lithic lapilli of pneumatic equivalence to the accretionary lapilli are abundant in the valley-fill ignimbrites, but they are absent in the thin ash veneers, which also contain the accretionary lapilli. Clearly, the competence of the current (measure of the largest-size clast a current is able to transport) on interfluves was insufficient to transport lapilli-sized clasts, and yet the veneer ignimbrites nevertheless contain abundant accretionary lapilli. At Montaña Magua, depochrons marking the appearance and disappearance of accretionary lapilli in Flow-unit 4 are ~0.6 m apart in veneer ignimbrite, but they are more than 12 metres apart in adjacent coeval massive valley-fill ignimbrite (Fig. 7). This indicates that depositional aggradation rates were ~20 times greater in the valleys than on the ridges. However, assuming that accretionary lapilli fell out of upper parts of the current into the aggrading ignimbrite across valleys and ridges, then there is a discrepancy between the thickness ratio of valley-fill and veneer ignimbrite (~1:20) and the accretionary lapilli concentration ratio (1:10). This can be accounted for by the common scours in veneer ignimbrite that indicate intermittent erosion. Thus, while ignimbrite was aggrading within valleys, ignimbrite on the interfluves underwent periodic deposition and erosion by the current.

The lateral variations in lithofacies between valley-fill and veneer ignimbrites exhibited by later deposited parts of Flow-unit 4 (Members 7–9; Fig. 7D) are considerably less marked than those exhibited by the earlier flow-units. This change was the result of: (A) a reduction in the relief and accommodation space provided by the valleys due to partial filling by the earlier ignimbrite flow-units; and (B) a marked increase in the volume of the fourth PDC. The increase in volume meant that the remaining topographic relief provided by the interfluves between the partly filled valleys failed to penetrate so high into the now thicker current's density-stratification, such that the more concentrated (granular fluid) lower levels of the current flowed more extensively across the interfluves. Nevertheless, particle concentrations in the lower levels of the current on the interfluves were not sufficiently high to entirely suppress turbulence, as recorded by diffuse bedding and stratification in the veneer facies of Member 7, in contrast with the entirely massive fills in the valleys. Conservation of mass requires that lateral spreading of the current across interfluves would affect the concentration-profile of the current at those locations, for example with thinning of the granular-fluid in lowermost levels of the current. Thus, the character of the lower flow-boundary zone of the current may have changed laterally with fluid-escape dominated deposition along the valleys, to form the massive lapilli-tuff at valley axes, and with less steady deposition more affected by granular flow and tractional processes across the interfluves, as recorded by the more variable, variously diffuse-stratified veneers (e.g., Branney and Kokelaar 2002).

Similar lateral variations in a large density current are recorded in the ignimbrite sheet of the 1991 eruption of Mount Pinatubo, Philippines (Scott et al. 1996), which also inundated radiating valleys and broad interfluves.

Depositional records of bypassing currents: sediment traps on the flanks of Las Cañadas volcano

Enhanced deposition from density currents on the stoss-side of topographic obstructions is common (e.g. Bursik and Woods 2000) and results from local decelerations, in some cases accompanied by the development of upstream propagating bores within the blocked, lower parts of density stratified currents (see Bursik and Woods 2000). The local current decelerations (depletive flow) will locally decrease the flow capacity. On southern flanks of Tenerife, thick ignimbrite accumulations developed upstream of scoria cones, which acted as 'sediment traps'. We infer that the high-concentration basal parts of the current were forced to slow, pond and flow around the sides of the cone (e.g., Baines 1995; Bursik and Woods 2000), while higher, less dense and turbulent levels of the current decoupled (sensu

Fisher 1995) and flowed across the cone, eroding the substrate, bypassing, or depositing thin ash veneers on the lee side.

In the broad Güimar valley, ignimbrite is absent within the Poris Formation on flat ground away from the scoria cones (logs A and E on Fig. 9). Either the Poris PDC did not flow across these regions or it remained non-depositional and bypassed where not blocked by topographic obstacles. However, the local presence of ignimbrite upstream of several scoria cones indicates that the density current accelerated down the steep east-facing scarps of the valley (>35° 1600 m high, Fig. 9) and then fanned out across the valley bottom. Across most of the valley floor the current remained non-depositional (logs A and E on Fig. 9) and passed out to sea. The current here deposited ignimbrite only where it was forced to slow and flow around scoria cones. Bypassing of PDCs over short distances (<5 km) is common on steep-sided composite volcanoes (e.g., Mount Misery, St. Kitts, Robool et al. 1987; Mount Pinatubo, Philippines, Scott et al. 1996; Roccamonfina volcano, Italy, Giordano 1998). Bypassing over greater distances (> 30 km) is rarer but was inferred to have occurred during large-magnitude eruptions such as the Campanian Ignimbrite, Italy (Fisher et al. 1993). During hazard surveys it would seem appropriate to target scoria cones or other traps on potential bypass surfaces in order to search for local ignimbrite accumulations that would record the passage of large currents: this could help construct eruption histories and determine the hazards around large explosive volcanoes.

Using longitudinal ignimbrite architecture to understand large-scale eruption dynamics

Longitudinal architectures in ignimbrite sheets are useful for deciphering large-scale eruption dynamics and regional-scale PDC behaviour (De Rita et al. 1998; Branney and Kokelaar 2002). Two conceptual models have been proposed to account for retrogradation architectures in ignimbrite sheets (Branney and Kokelaar 2002): (1) extending aggradation with dual onlap, such as may result from waxing flow, or (2) overall retrogradation, such as may result when runout distance decreases during waning flow (Fig. 11A). In the former model, the geographic area of deposition increases with time, creating onlap architectures in proximal areas mirrored by onlap in more distal areas; and may result from overall waxing flow. In the latter model, onlap upslope in proximal areas is accompanied by offlap in distal areas as the distal limit of deposition decreases with time, recording a gradual decrease in runout distance with time, such as may occur due to overall waning flow conditions. The distal architecture of the Poris ignimbrite sheet is obscured by the sea, but from subaerial exposures alone it is apparent that neither of these models fits perfectly. This is because the field relations indicate that retrogradation occurred during strongly waxing flow (see Fig. 5, 6 and 11B; see also Brown and Branney 2004b), as indicated by the overall upward-coarsening sequence, from tuff at the base of Flow-unit 1 to lithic breccias high in Flow-unit 4, (thought to record peak flow conditions as the caldera subsided), and also by the overall increase in geographic area covered by the currents with time. The lower flow-units (1-3) are geographically restricted and preserve in-situ fossil shrubs at their bases, whereas Flow-unit 4 is more widespread and contains abundant allochthonous tree trunks and entrained locally-derived lithic clasts, and coarsens upward into an extensive lithic breccia (see Brown and Branney 2004b). These features suggest that the capacity, competence and the dynamic pressure of the current increased with time during the Poris eruption. The lithic breccia high in Flow-unit 4 is a particularly widespread unit and probably records peak flow conditions (Brown and Branney 2004a). Thus, the retrogradational architecture that is widely exhibited within the Poris ignimbrite sheet across southern Tenerife was assembled during predominantly waxing flow conditions.

We propose that where the current flowed onto lower slopes it was critically balanced with respect to deposition: that is, substantive accelerations within the current were close to zero (autosuspension) because the waxing mass-flux of the current was balanced by depletive flow on the gentle concave slope. In this condition even a very small change in topography was sufficient to locally push the current into deposition (substantive deceleration). Thus, rather minor slope-changes induced slight spatial decelerations sufficient to trigger the onset of deposition in a restricted (~50 m reach) depositional zone. Downcurrent of this zone, the slope was unchanged and the current bypassed to the ocean. Soon, however, the location of the minor slope-induced deposition shifted upcurrent because the current now had to flow over the newly formed ≤5 m-thick lens of deposit. Downslope of the lens crest the current continued to flow away downslope to the ocean, without depositing (bypassing). The new deposit lens now itself caused the local deceleration (depletive flow) causing the zone of deposition to shift sourceward, depositing a new lens and so on, so that over time (hours) a single, extensive layer (2–5 m thick over interfluves and <20 m thick along valley axes) was gradually assembled retrogradationally during the eruption. As the eruption waxed, new additions to this layer were coarser-grained (e.g. lithic breccia). Thus we infer that the retrogradation exhibited widely by the Poris and other ignimbrite sheets in southern Tenerife resulted from the gentle concave regional slope and not due to waning flow.

Rates of deposition on this gentle concave slope remained low when compared with the inferred larger volumes of material that passed by. This is in contrast with more rapid deposition at a marked break-of-slope as described elsewhere where wholesale rapid deposition is caused by abrupt deceleration with or without a hydraulic jump at a steep obstacle or major change in slope. Eventually, as flow peaked the zone of deposition broadened with aggradation of a new layer of lithic breccia overlapping the earlier retrogradational components of the sheet (Fig. 11C). Locally, the peak waxing phase was sufficient to cause erosion and entrainment of just-deposited ignimbrite, stripping up to 4 m of just-deposited ignimbrites).

The presence of a widespread clast-supported pumice-rich ignimbrite (Member 9, Fig. 3) capping Flow-unit 4 is consistent with retrogradation of the ignimbrite sheet, this time as the eruption waned after the caldera-collapse climax. These pumice concentrations are thought to have formed when buoyant large pumice clasts overpassed to become deposited near the distal limits of the current, leaving typical clast-supported pumice-accumulations (snouts and levees). During the sustained current's waning, the distal limits of the current retracted sourceward (retrogradation), producing a strand-line of pumice deposits preserved in uppermost parts of the resultant ignimbrite sheet. This mechanism accounts for upper pumice concentrations in zoned ignimbrites elsewhere (e.g. Zaragoza ignimbrite, Carrasco-Nuñez and Branney 2005). The last upslope lens deposited during final waning stages of the current left a 2-m high dam that after the eruption collected water forming a small lake in which 2 m of pumiceous sediments accumulated (Branney and Brown 2004a), showing that the upslope limit of the present ignimbrite sheet represents the true preserved original limit, not an eroded remnant.

In summary, the longitudinal retrogradational architecture of the onshore Poris ignimbrite sheet (see Fig. 11C) resulted primarily from the gently concave regional slope, and occurred during both overall waxing flow conditions (coarsening upwards) and during late-stage waning flow conditions (recorded by upper lithic-poor pumice accumulations). As the last, more prolonged current waxed to the climactic phase, earlier-deposited parts of the ignimbrite were locally stripped out by vigorous erosion, and during the climactic phase of the current (as the caldera collapsed; Brown and Branney 2004a) a second layer of ignimbrite was widely assembled above the earlier, retrogradational part of the ignimbrite. This layer was characterised by widespread lithic breccias.

Conclusions

Cryptic internal architectures within an extensive ignimbrite sheet on Tenerife have revealed how conditions within a widespread, sustained PDC varied spatially (due to the influence of the regional slope and local valleys and obstacles) and with time (as a result of changing eruption dynamics and modification of topography by deposition). During a large Plinian eruption four widespread, sustained pyroclastic density currents swept down the broadly concave flanks of Las Cañadas volcano.

(1) The overall gentle concavity of the volcano’s flanks controlled where the currents deposited on a regional scale. The currents bypassed the steeper upper flanks and began to deposit as the slopes gradually decreased with proximity to the coast, more than 15 km from the source caldera. Deposition occurred during both waxing and waning flow periods, and so is inferred to have resulted predominantly from topography-induced spatial deceleration (depletive flow) caused by the combination of slightly divergent flow (flow-paths fanning out) and passage onto lower gradients.

(2) Bypassing (flow without deposition) characterised PDC behaviour for the majority of the runout distance. The flanks of Cañadas volcano behaved as a broad ‘chute’ or bypass surface, conveying most of the erupted material to the ocean, more than 15 km from source. Such PDC behaviour has two consequences: (A) the volume of the ignimbrite eruptions on Tenerife is difficult to estimate because the bulk of the material resides offshore, so eruption volumes far exceed the volumes of onshore deposits; and (B) it is liable to lead to under-estimates of the number of hazardous density currents to have passed across a volcano flank, because such currents widely leave no depositional record of their passage. Thus, to estimate the true number of density currents that have crossed an area requires careful piecing-together of incomplete information from scattered patches of deposit. This is unlikely to be achieved where exposure is less superlative than is the case in the southern Tenerife desert.

(3) The prolonged nature (and hence large volume) of a pyroclastic density current that was sustained, for example, throughout the entire duration of a caldera-collapse phase of a large explosive eruption (e.g. Poris Flow-unit 4) may not be immediately apparent from a deceptively thin ignimbrite flow-unit. The thinness of the ignimbrite on a gently concave volcano flank is the result of limited accommodation space (topography), not the duration or size of the current, which may have been prolonged. At any one location deposition occurred during just a fraction of the flow’s duration across that location.

(4) On gently concave slopes, ignimbrite flow-units were assembled incrementally by upslope advance of the deposit’s source-facing feather-edge. The deposition was diachronous, and the resultant retrogradational onlap architecture within the ignimbrite flow-unit is developed both within the valley fills and in the thin ignimbrite veneers. However, whereas in the veneers, this architecture can be apparent from diffuse-bedding with low-angle backset-type geometry, the same architecture can be entirely cryptic within massive, thicker valley-filling ignimbrite, and only revealed there by analysis of the compositional zoning.

(5) Local obstacles, such as scoria cones on the bypass surface acted as sediment traps by inducing local depletive conditions with consequent localised deposition of ignimbrite from currents that left little record elsewhere. When attempting fieldwork reconstructions of the PDC history of a large explosive volcano, targeting of stoss sides of scoria cones for investigation is a rewarding strategy

(6) Deposition of ignimbrite by a sustained PDC modifies the substrate topography sufficiently rapidly to alter the current's spatial patterns of deposition and erosion. In hazard models that predict density current dispersals, assumptions of a constant (e.g. DEM) topography during an eruption may yield misleading results in the case of sustained currents.

(7) The Poris PDCs were concentrated (granular-fluid based) and density-stratified, as revealed by the field relations across the margins of flow-parallel valleys. Lower, granular-fluid levels of the earlier, smaller currents were largely channelled within pre-existing valleys, whereas higher, more dilute levels spilled widely across extensive interfluves, leaving finer-grained veneers. In contrast, the larger current that deposited Flow-unit 4 flowed across a landscape in which topographic irregularities had been substantially dampened by deposition of ignimbrite from the earlier PDCs. The lower, granular-fluid levels of this current flowed widely across both valleys and interfluves, although the competence of the current to transport large clasts was somewhat higher along valley axes than it was along the elevated interfluves. This PDC was sustained before, during, and after the climactic caldera collapse phase of the eruption, and its grainsize variations record the waxing flow, peak flow, and waning flow conditions. Topography-induced depletive flow was locally sufficiently marked to induce deposition even during the initial phase of waxing flow. However, at several locations the current eroded and entrained several metres thickness of loose ignimbrite deposited by the same current earlier during its waxing phase. This widespread removal of lower parts of Flow-unit 4 means that many sections are incomplete, and record just peak flow and subsequent phases of the current.

The presented data illustrate how variations in PDC dispersal, onlapping relationships, diachronous surfaces, bypassing and the waxing and waning of individual currents and of the eruption overall mean that any single vertical section through an ignimbrite sheet may record just a fraction of the complete eruption sequence. Failure to recognise this during hazard assessments may lead to under-estimations of PDC volumes, dispersals and frequencies. This may be most critical on ocean island volcanoes where subaerial flanks act as bypass surfaces across which the PCDs convey the majority of their load into the sea. However, where exposure is sufficient, and by targeting local sediment traps such as stoss sides of scoria cones, more complete flow-histories can be carefully pieced together from patchy deposits, particularly where reconstructions are aided by compositional zoning of the ignimbrite.

Acknowledgements

We thank Natasha Smith, Peter Kokelaar, Pablo Dávila-Harris, Steve Self and Jan Zalasiewicz for many useful discussions. We thank Brittany Brand and Roberto Sulpizio for critical reviews that greatly improved the manuscript and Michael Manga for reviews and editorship.

References

Alexander J, Morris M (1994) Observations on experimental, non-channelized, high-concentration turbidity currents and variations in deposits around obstacles. J Sed Res A64:899-909

Allen SR, Cas RAF (1998) Lateral variations within coarse co-ignimbrite lithic breccias of the Kos Plateau Tuff, Greece: Bull Volcanol 59:356-377

Amy LA, Kneller BC, McCaffrey WD (2007) Facies architecture of the Grès de Peïra cava, SE France: Landward stacking patterns in ponded turbidite basins. J Geol Soc 164:143-162

Ancochea E, Fuster JM, Ibarrola E, Cendrero A, Coello J, Hernan F, Cantagrel JM, Jamond C (1990) Volcanic evolution of the island of Tenerife (Canary Islands) in the light of new K-Ar data: J Volcanol Geotherm Res 44:231-249

Ancochea E, Huertas MJ, Cantagrel JM, Coello J, Fuster JM, Arnuad N, Ibarrola E (1999) Evolution of the Cañadas edifice and its implications for the origin of the Cañadas Caldera (Tenerife, Canary Islands): J Volcanol Geotherm Res 88:177-199

Andrews GDM, Branney MJ (2011) Emplacement and rheomorphic deformation of a large, lava-like rhyolite ignimbrite: Grey's Landing, southern Idaho. Geol Soc Am Bull 123:725-743

Andrews BJ, Manga M (2011) Effects of topography on pyroclastic density current runout and formation of co-ignimbrites. Geology 39:1099-102

Andrews BJ, Manga M (2012) Experimental study of turbulence, sedimentation, and co-ignimbrite mass partitioning in dilute pyroclastic density currents. J Volcanol Geotherm Res 225-226:30-44

Baines PG (1995) Topographic effects on stratified flows. Cambridge University Press, 482 pp

Best JL, Kostaschuk RA, Peakall J, Villard PV, Franklin M (2005) Whole flow field dynamics and velocity pulsing within natural sediment-laden underflows. Geology 33:765-768

Bogaard P (1998) $^{40}Ar/^{39}Ar$ ages of Pliocene-Pleistocene fallout tephra units and volcaniclastic deposits in the sedimentary aprons of Gran Canaria and Tenerife (sites 953, 954 and 956). Proc Ocean Drilling Program, Sci Res 157:329-41.

Bourdier J, Abdurachman EK (2001) Decoupling of small-volume pyroclastic flows and related hazards at Merapi volcano, Indonesia. Bull Volcanol 63:309-325

Branney MJ, Kokelaar BP (1992) A reappraisal of ignimbrite emplacement: progressive aggradation and changes from particulate to non-particulate flow during emplacement of high-grade ignimbrite. Bull Volcanol 54:504-520

Branney MJ, Kokelaar BP (1994) Volcanotectonic faulting, soft-state deformation and rheomorphism of tuffs during development of a piecemeal caldera, English Lake District. Geol Soc Am Bull 109:507-530

Branney MJ, Kokelaar BP (1997) Giant bed from a sustained catastrophic density current flowing over topography: Acatlan ignimbrite, Mexico. Geology 25:115-118

Branney MJ, Kokelaar P (2002) Pyroclastic density currents and the sedimentation of ignimbrites. Geol Soc London Memoir 27:1-152

Branney MJ, Barry TL, Godchaux M (2004) Sheathfolds in rheomorphic ignimbrites. Bull Volc 66:485-491

Brown RJ, Barry TL, Branney MJ, Pringle MS, Bryan SE (2003) The Quaternary pyroclastic succession of southern Tenerife, Canary Islands: explosive eruptions, related subsidence and sector collapse. Geol Mag 140:265-288

Brown RJ, Branney MJ (2004a) Event-stratigraphy of a caldera-forming ignimbrite eruption on Tenerife: the 273 ka Poris Formation. Bull Volcanol 66:392-416

Brown RJ, Branney MJ, (2004b) Bypassing and diachronous deposition from pyroclastic density currents: evidence from a giant regressive bedform (Poris Formation, Tenerife). Geology 32:445-448

Brown RJ, Branney MJ, Maher C, Dávila-Harris P (2010) Origin of accretionary lapilli within ground-hugging density currents: Evidence from pyroclastic couplets on Tenerife. Bull Geol Soc Am 122:305-320

Brown RJ, Bonadonna C, Durant AJ (2012) A review of ash aggregation. Phys Chem Earth 45-46:65-78

Bryan SE, Marti J, Cas RAF (1998a) Stratigraphy of the Bandas del Sur Formation: an extracaldera record of Quaternary phonolitic explosive volcanism from the Las Cañadas edifice, Tenerife (Canary Islands). Geol Mag 135:605-636

Bryan SE, Marti J, Cas RAF (1998b) Lithic breccias in intermediate volume phonolitic ignimbrites, Tenerife (Canary Islands): constraints on pyroclastic flow depositional processes. J Volcanol Geotherm Res 81:269-296

Bryan SE, Marti J, Cas RAF, Marti J (2000) The 0.57 Ma Plinian eruption of the Granadilla Member, Tenerife (Canary Islands): an example of complexity in eruption dynamics and evolution. J Volcanol Geotherm Res 103:209-238

Burgisser A, Bergantz GW (2002) Reconciling pyroclastic flow and surge: The multiphase physics of pyroclastic density currents. Earth Planet Sci Lett 202:405-418

Bursik MI, Woods AW (2000) The effects of topography on sedimentation from particle-laden turbulent density currents. J Sed Res 70: 53-63

Calder ES, Cole PD, Dade WB, Druitt TH, Hoblitt RP, Huppert HE, Ritchie L, Sparks RSJ, Young SR (1999) Mobility of pyroclastic flows and surges at the Soufriere Hills Volcano, Montserrat. Geophys Res Lett 26:537-540

Carrasco-Núñez G, Branney MJ (2005) Progressive assembly of a massive layer of ignimbrite with normal-to-reverse compositional zoning: the Zaragoza ignimbrite of central Mexico. Bull Volcanol 68: 3-20

Choux CM, Druitt TH (2002) Analogue study of particle segregation in PDCs, with implications for the emplacement mechanisms of large ignimbrites. Sedimentology 49:907-928

Dade WB, Huppert HE (1996) Emplacement of the Taupo ignimbrite by a dilute, turbulent flow: Nature 381:509-512

Dávila Harris P (2009) Explosive ocean-island volcanism: the 1.8–0.7 Ma explosive eruption history of Cañadas volcano recorded by the pyroclastic successions around Adeje and Abona, southern Tenerife, Canary Islands. Unpub PhD thesis, Univ Leics, UK

Dávila Harris P, Branney MJ, Storey M (2011) Large eruption-triggered ocean-island landslide at Tenerife: Onshore record and long-term effects on hazardous pyroclastic dispersal. Geology 39:951-954

Dávila Harris P, Ellis BS, Branney MJ, Carrasco-Nunez G (in press) Physical volcanology and geochemistry of a vitric spatter-bearing ignimbrite: the Quaternary Adeje Formation, Cañadas volcano, Tenerife. Bull Volcanol

Dellino et al., 2007. 2010

Denlinger RP, Iverson RM (2001) Flow of variably fluidized granular masses across three dimensional terrain, 2. Numerical predictions and experimental texts. J Geophys Res 106:553-566

De Rita D, Giordano G, Milli S (1998) Forestepping-backstepping stacking patterns of volcaniclastic successions: Roccamonfina volcano, Italy. J Volcanol Geotherm Res 80:155-178

Doronzo DM, Valentine GA, Dellino P, de Tullio MD (2010) Numerical analysis of the effect of topography on deposition from dilute pyroclastic density currents. Earth Planet Sci Lett 300:164-73

Doronzo DM, Dellino (2012) Interaction between pyroclastic density currents and buildings: Numerical simulation and first experiments. Earth Planet Sci Lett 310:286-292

Druitt TH (1998) Pyroclastic density currents: In: Gilbert JS, Sparks RSJ (Eds) The Physics of explosive eruptions. Geol Soc London Spec Pub 145:145-182

Druitt TH, Calder E, Cole PD, Hoblitt RP, Loughlin S, Norton GE, Ritchie LJ, Sparks RSJ, Voight B (2002) Small-volume, highly mobile pyroclastic flows formed by rapid sedimentation from pyroclastic surges at Soufriere Hills Volcano, Montserrat: an important volcanic hazard. In: Druitt TH, Kokelaar BP (Eds) The eruption of Soufrière Hills Volcano, Montserrat. Geol Soc London Memoir 21:263-279

Dufek J, Wexler J, Manga M (2009) Transport capacity of pyroclastic density currents: Experiments and models of substrate-flow interaction. J Geophys Res 11:DOI: 10.1029/2008JB006216

Edgar CJ, Wolff JA, Nichols HJ, Cas CAF, Marti J (2002) A complex quaternary ignimbrite-forming phonolite eruption: the Poris Member of the Diego Hernandez Formation (Tenerife, Canary Islands): J Volcanol Geotherm Res 118:99-130

Fierstein J, Hildreth W (1992) The Plinian eruptions of 1912 at Novarupta, Katmai National Park, Alaska. Bull Volcanol 54:646-684

Fierstein J, Wilson CJN (2005) Assembling an ignimbrite: Compositionally defined eruptive packages in the 1912 Valley of Ten Thousand Smokes ignimbrite, Alaska. Bull Geol Soc Am 117:1094-1107

Fisher RV (1966) Mechanism of deposition from pyroclastic flows. Am J Sci 264:350-363

Fisher RV (1990) Transport and deposition of a pyroclastic surge across an area of high relief – the 18 May 1980 eruption of Mount St. Helens, Washington. Geol Soc Am Bull 102:1038-1054

Fisher RV, Orsi G, Ort M, Heiken G (1993) Mobility of a large-volume pyroclastic flow – emplacement of the Campanian ignimbrite, Italy. J Volcanol Geotherm Res 56:205-220

Fisher RV (1995) Decoupling of pyroclastic currents - hazards assessment: J Volcanol Geotherm Res 66:257-263

Garcia MH, Parker G (1989) Experiments on hydraulic jumps in turbidity currents near a canyon-fan transition. Science 245:393-396

Gertisser R, Cassidy NJ, Charbonnier SJ (2012) Overbank block-and-ash flow deposits and the impact of valley-derived, unconfined flows on populated areas at Merapi volcano, Java, Indonesia. Nat Haz 60:623-648

Giordano G (1998) Facies characteristics and magma-water interaction of the White Trachytic Tuffs (Roccamonfina Volcano, Southern Italy). Bull Volcanol 60:10-26

Girolami L, Roche O, Druitt TH, Corpetti T (2010) Velocity fields and depositional processes in laboratory ash flows. Bull Volcanol72:747-759, doi:10.1007/s00445-010-0356-9

Gray TE, Alexander J, Leeder MR (2005) Quantifying velocity and turbulence structure in depositing sustained turbidity currents across breaks in slope. Sedimentology 54:467-488 dpi 10.1111/j.1365-3091.2005.00705.x

Gurioli L, Sulpizio R, Cioni R, Sbrana A, Santacroce R, Luperini W, Andronico D (2010) Pyroclastic flow hazard assessment at Somma-Vesuvius based on geological record. Bull Volcanol 72:1021-1038

Hiscott RN (1994) Loss of capacity, not competence, as the fundamental process governing deposition from turbidity currents. J Sed Res 64:209-214

Huertas MJ, Arnaud NO, Ancochea E, Cantagrel JM, Fúster JM (2002) $^{40}Ar/^{39}Ar$ stratigraphy of pyroclastic units from the Cañadas volcanic edifice (Tenerife, Canary Islands) and their bearing on the structural evolution. J Volcanol Geotherm Res 115:351-365

Kassem A, Imran J (2001) Simulation of turbid underflows generated by the plunging of a river. Geology 29:655-659

Kneller B, Edwards D, McCaffrey W, Moore R (1991) Oblique reflection of turbidity currents. Geology 19:250-252

Kneller B, Branney MJ (1995) Sustained high-density turbidity currents and the deposition of thick massive sands. Sedimentology 42:607-617

Kneller B, McCaffrey W (1999) Depositional effects of flow non-uniformity and stratification within turbidity currents approaching a bounding slope: Deflection, reflection, and facies variation. J Sed Res 69:980-991

Kokelaar P (1992) Ordovician marine volcanic and sedimentary record of rifting and volcanotectonics. Snowdon, Wales, United Kingdom. Bull Geol Soc Am 104:1433-1455

Komar PD (1971) Hydraulic jumps in turbidity currents. Geol Soc Am Bull 82:1477-1488

Kröchert J, Buchner E (2009) Age distribution of cinder cones within the Bandas del Sur formation, southern Tenerife, Canary Islands. Geol Mag146:161-172

Kubo Y (2004) Experimental and numerical study of topographic effects on deposition from two-dimensional, particle-driven density currents. Sediment Geol 164:311-26.

Legros F, Kelfoun K (2000) On the ability of pyroclastic flows to scale topographic obstacles. J Volcanol Geotherm Res 98:235-241

Lirer L, Petrosino P, Alberico I, Postiglione I (2001) Long-term volcanic hazard forecasts based on Somma-Vesuvio past eruptive activity. Bull Volcanol 63:45-60

Loughlin SC, Calder ES, Clarke A, Cole PD, Luckett R, Mangan MT, Pyle DM, Sparks RSJ, Voight B, Watts RB (2002) Pyroclastic flows and surges generated by the 25 June 1997 dome collapse, Soufrière Hills volcano, Montserrat. In: Druitt TH, Kokelaar BP (Eds) The eruption of Soufrière Hills Volcano, Montserrat. Geol Soc London Memoir 21:181-209

Lube G, Cronin SJ, Thouret JC, Surono (2011) Kinematic characteristics of pyroclastic density currents at Merapi and controls on their avulsion from natural and engineered channels. Geol Soc Am Bull 123:1127-1140

Macías JL, Espíndola JM, Bursik M, Sheridan MF (1998) Development of lithic-breccias in the 1982 pyroclastic flow deposits of El Chichón volcano, Mexico. J Volcanol Geotherm Res 83:173-196

Morris SA, Alexander J (2003) Changes in flow direction at a point caused by obstacles during passage of a density current. J Sediment Res 73:621-629

Marti J, Mitjavila J, Arana V (1994) Stratigraphy, structure and geochronology of the Las Cañadas caldera (Tenerife, Canary Islands) Geol Mag 131:715-727

Mulder T, Alexander J (2001) Abrupt change in slope causes variation in the deposit thickness of concentrated particle-driven density currents. Mar Geol 175:221-235

Pittari A, Cas RAF, Edgar CJ, Nichols HJ, Wolff JA, Marti J (2006) The influence of palaeotopography on facies architecture and pyroclastic flow processes of a lithic-rich ignimbrite in a high gradient setting: The Abrigo ignimbrite, Tenerife, Canary Islands. J Volcanol Geotherm Res 152:273-315

Robool MJ, Smith AL, Wright JV (1987) Lithic breccias in pyroclastic flow deposits on St. Kitts, West Indies. Bull Volcanol 49:694-707

Roche O, Gilbertson MA, Phillips JC, Sparks RSJ (2005) Inviscid behaviour of fines-rich pyroclastic flows inferred from experiments on gas-particles mixtures. Earth Planet Sci Lett 240:401-414 doi:10.1016/j.epsl.2005.09.053.

Roche O, Atalli, M, Mangeney A, Lucas A (2011) On the run-out distance of geophysical gravitational flows: insight from fluidized granular collapse experiments. Earth Planet Sci Lett 311:375-385, doi: 10.1016/j.epsl.2011.09.023

Roche O (2012) Depositional processes and gas pore pressure in pyroclastic flows: an experimental perspective. Bull Volcanol 74:1807-1820, doi: 10.1007/s00445-012-0639-4

Rossano S, Mastroloronzo G, De Natale G (2004) Numerical simulation of pyroclastic density currents on Campi Flegrei topography: a tool for statistical hazard estimation. J Volcanol Geotherm Res 132:1-14

Schumacher R, Schmincke H-U (1990) The lateral facies of ignimbrites at Laacher See volcano. Bull Volcanol 52:271-285

Scott WE, Hoblitt RP, Torres RC, Self S, Martinez ML, Nillos TJ (1996) Pyroclastic flows of the June 15 1991, climactic eruption of Mount Pinatubo. In: Newhall CG, Punongbayan S (Eds) Fire and Mud: eruptions of Pinatubo, Philippines. Philippine Institute of Volcanology and Seismology, Quenzen City. University of Washington Press, Seattle, 545-570

Smith N (2012) Near-vent processes of the 273 ka Poris eruption (Tenerife). Unpublished PhD Thesis, Univ Liverpool

Sohn YK (1997) On traction-carpet sedimentation. J Sed Res 67:502-509

Stevenson CJ, Talling PJ, Wynn RB, Masson DG, Hunt JE, Frenz M, Akhmetzhanhov A, Cronin BT (2013) The flows that left no trace: very large-volume turbidity currents that bypassed sediment through submarine channels without eroding the sea floor. Mar Pet Geol 41:186-205

Sulpizio R, Mele D, Dellino P, La Volpe L (2007) Deposits and physical properties of pyroclastic density currents during complex Subplinian eruptions: the AD 472 (Pollena) eruption of Somma Vesuvius, Italy. Sedimentology 54:607-635

Sulpizio R, Dellino P (2008) Sedimentology, depositional mechanisms and pulsating behaviour of pyroclastic density currents. In: Gottsmann J, Marti J, (Eds) Caldera volcanism: analysis, modelling and response. Developments in Volcanology 10:57-96, Elsevier, Amsterdam

Sulpizio R, De Rosa R, Donato P (2008) The influence of variable topography on the depositional behaviour of pyroclastic density currents: The examples of the Upper Pollena eruption (Salina Island, southern Italy). J Volcanol Geotherm Res 175:367-385

Sulpizio R, Bonasia R, Dellino O, Mele D, Di Vito MA, La Volpe L (2010) The Pomici di Avellino eruption of Somma-Vesuvius (3.0 ka BP). Part II: sedimentology and physical volcanology of pyroclastic density current deposits. Bull Volcanol 72:559-577

Valentine GA (1987) Stratified flow in pyroclastic surges. Bull Volcanol 49:616-630

Valentine GA, Wohletz KH, Kieffer SW (1992) Effects of topography on facies and compositional zonation in caldera-related ignimbrites: Geol Soc Am Bull 104:154-165

Van Andel TH, Komar PD (1969) Ponded sediments of the Mid-Atlantic ridge between 22 and 23 North. Geol Soc Am Bull 80:1163-1190

Van Eaton AR, Wilson CJN (2013) The nature, origins and distribution of ash aggregates in a large-scale wet eruption deposit: Oruanui, New Zealand. J Volcanol Geotherm Res 250:129-154

Walker GPL, Wilson CJN, Froggatt PC (1981) An ignimbrite veneer deposit—the trail marker of a pyroclastic flow. J Volcanol Geotherm Res 9:409–421

Watts AB, Masson DG (2001) New sonar evidence for recent catastrophic collapses of the north flank of Tenerife, canary islands. Bull Volcanol 63:8-19

Wilson CJN, Walker GPL (1985) The Taupo Eruption, New Zealand: II. The Taupo Ignimbrite. Phil Trans Roy Soc London, Series A-Math Phys Eng Sci 314:229-310

Wilson CJN (2001) the 26.5 ka Oruanui eruption, New Zealand: an introduction and overview. J Volcanol Geotherm Res 112:133-174

Woods AW, Bursik MI, Kurbatov AV (1998) The interaction of ash flows with ridges. Bull Volcanol 60:38-51

Figure Captions

Figure 1. Map of south Tenerife with the major outcrops of the Poris Formation marked. Delineated areas refer to regions referred to in later figures. DEM from GRAFCAN (www.grafcan.es).

Figure 2. DEM of Tenerife shaded for slope angle. Note the crescent-shaped region of low gradient slopes along the southern coast where most of the Poris ignimbrites were deposited (the Bandas del Sur region). Inset shows representative slope profiles as marked on map.

Figure 3. Generalised and composite vertical section of the Poris Formation as exposed along the southern coast of Tenerife with summary of the main characteristics of the members. Taken from Brown and Branney (2004b). L – lapillistone; LT – lapilli tuff; acc – accretionary lapilli; pel - ash pellets; p – pumice-rich; l – lithic-rich; m – massive; db – diffuse-bedded; s – stratified; xs – cross-stratified. See Brown and Branney (2004b) for a full description of members and lithofacies.

Figure 4. Distribution of ignimbrite flow-units across the southern flank of Tenerife. Representative measured sections through the Poris Formation illustrating the distribution and thickness variations of flow-units. Inset DEM of Tenerife showing the minimum areas of the island inundated by successive PDCs. The dispersal of PDCs increased with time during the eruption. Cartoon illustrating the dispersal of the four flow-units in the Poris Formation (see Fig. 1 for localities).

Figure 5. Parallel-to-current architecture of the Poris ignimbrite sheet at Montaña Magua (Fig. 1). Measured sections through the ignimbrite sheet indicate that the flow-units, and members in Flow-unit 4, pinch-out upslope against the substrate. Thus the base of the ignimbrite sheet is diachronous. Logs compressed for clarity: inset shows the location of measured sections and a restored longitudinal cross-section through the ignimbrite sheet.

Figure 6. Longitudinal architecture of the Poris ignimbrite sheet around Montaña Magua (see Fig 1 and inset in Fig 5). A) View downcurrent of Member 8 (Flow-unit 4) which onlaps upstream against the topographic slope (UTM: 357661/3119160). Member 7 (also of Flow-unit 4) in distance and preserved in small topographic depressions (arrowed). B) Member 7 pinching out upslope (UTM: 357945/3119059). C) Opposite side of valley to B. Bedding within Member 7 ignimbrite pinching out against the topographic slope. Current is from left to right. D) Lens of Member 9 ignimbrite overlain by volcaniclastic sands and gravels that were deposited against the upstream-dipping surface of the ignimbrite sheet. E) Member 8 lithic breccia forming the proximal feather edge of the ignimbrite sheet at El Arrecife. All lower units have pinched out further downslope. Current oblique out of page, left to right (UTM: 357654/3117857). F) Block diagram illustrating the reconstructed architecture of the ignimbrite sheet as based on outcrops around Montaña Magua (see Figs 5 and 7). Note the onlapping relationships of successive units and the retro-gradational, back-stepping architecture. F) Parallel-to-current section through the Abades ignimbrite showing onlapping of lithic-bearing layers (dashed lines) against the palaeoslope (arrowed). The base of the ignimbrite sheet is diachronous.

Figure 7. Representative logs at Montaña Magua through the ignimbrite sheet in veneer, valley-margin and valley-fill locations (for location see inset, Fig. 5). A) Panoramic view of spectacular palaeo-valley-filling ignimbrites. View to north and current out of page. Palaeo-valley axis runs out of the centre of the page (see inset in Fig. 5 for location). B) Close-up of northern valley-fill in B showing transition from valley-filling facies to veneer facies. Position of logs in A is indicated. Note that these

outcrops are being progressively covered by bulldozed rubble from adjacent construction work. C) Close-up of southern valley-fill in B showing abrupt pinch-out of valley-fill facies in Flow-unit 2. Flow-unit 2 was largely confined within the valley. D) Cartoon showing reconstructed transverse-to-current architecture across a palaeo-valley. Lithofacies as in Fig. 1 and Brown and Branney (2004b).

Figure 8. Interaction of PDCs with scoria cones on the southern flank of Tenerife. A) Photo of the Fasnia scoria cone (Fig. 1; UTM 359476/3123344), which has an anomalously stoss-side accumulation of Fasnia Formation ignimbrite; lee side is mantled by coeval thin ignimbrites and fall deposits. B) Anomalously thick ignimbrite on stoss side of Fasnia cone.

Figure 9. The interaction of PDCs and scoria cones in the Poris Formation. A) Measured sections through the Poris ignimbrite sheet in the Güimar valley (see inset for localities). Ignimbrite sheet is composed mostly of Flow-unit 4, which is thickest immediately upstream of the scoria cones, but is absent in localities away from the cones. PDCs generated in Las Cañadas caldera flowed into the Güimar valley on their way to the sea. Insets show location of sections. Aerial photograph 2011 Google ©.

Figure 10. Cartoon illustrating the different depositional regimes developed as PDCs disperse away from Las Cañadas caldera on Tenerife. In intra-caldera settings high ignimbrite accumulation rates resulted from topographic reflection and obstruction of PDCs by the growing caldera wall (A). In immediate extracaldera settings parts of the PDC that escaped the caldera rapidly sedimented thick ignimbrite over flat ground (B; see Smith and Kokelaar submitted). As the currents accelerated down the steep upper flanks of the flanks of the volcano they entered into an accumulative capacity and started to erode the substrate (C). They were effectively in a bypassing regime. Ignimbrite was not deposited except where parts of the current were obstructed by scoria cones (D). As they reached the lower flanks the currents passed onto lower gradient slopes, decelerated and entered into a depletive

capacity. This may have coincided with a hydraulic jump in the current. Loss of capacity resulted in ignimbrite deposition. The transition from a bypassing regime into a depositional regime is marked in the deposit by abundant stratification and scours within the deposit (E). Deceleration across the coastal flanks and out into the ocean resulted in rapid sedimentation rates (F).

Figure 11. Conceptual models for the architecture of the Poris ignimbrite sheet on the southern flank of Tenerife and interpretations of the gross eruption dynamics (following Branney and Kokelaar 2002). A) Two possible models to explain the genesis of the observed retrogradational, onlapping architecture of the proximal edge of the Ignimbrite sheet: extending aggradation with dual onlap (waxing mass-flux) or retrogradation (strongly waning flow). B) Cartoon qualitatively illustrating the changing mass flux of the Poris PDCs as deduced from lithological evidence in the ignimbrites. C) Preferred interpretation of the Poris ignimbrite sheet as inferred from both architecture and from lithological evidence—extending aggradational with dual onlap followed by retrogradation architecture resulted from an initial intermittent but low volume that increased rapidly during the eruption before strongly waning.

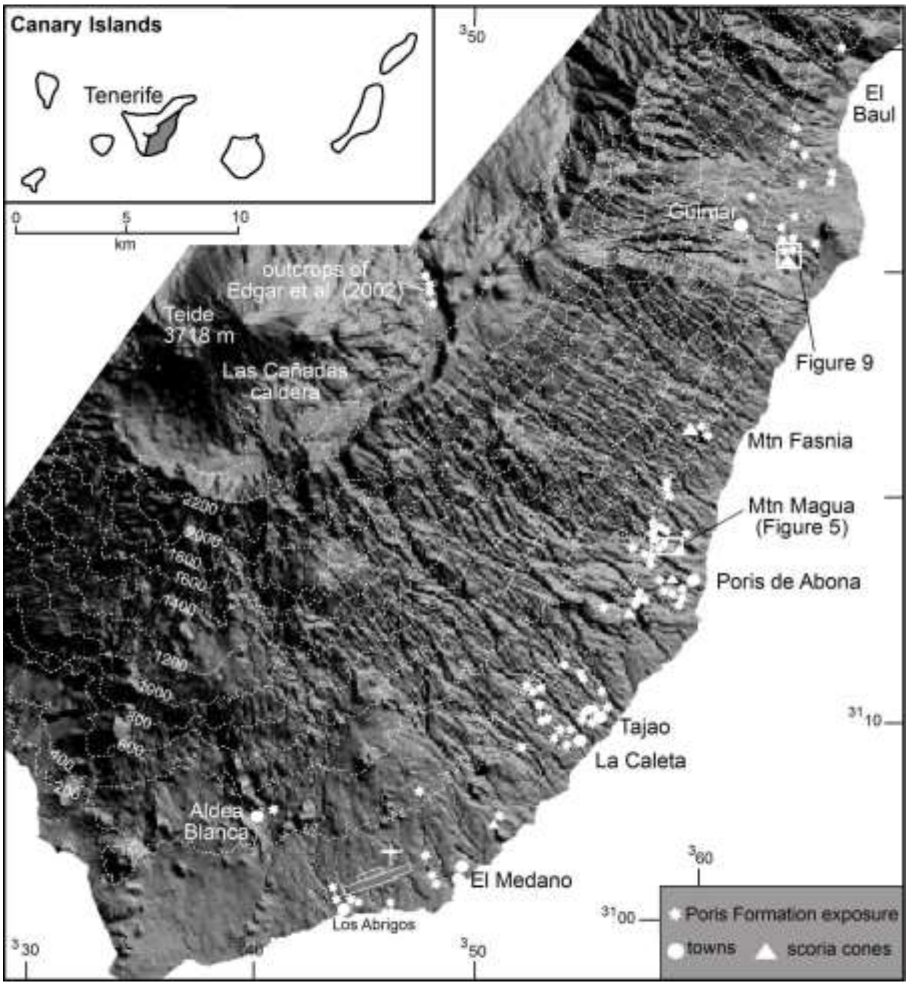

Canary Islands
Tenerife
0
5
10
km
$^{3}50$
El
Baul
Guimar
outcrops of
Edgar et al. (2002)
Teide
3718 m
Las Cañadas
caldera
Figure 9
Mtn Fasnia
Mtn Magua
(Figure 5)
Poris de Abona
2200
1200
400
200
Tajao
La Caleta
$^{31}10$
Aldea
Blanca
$^{3}60$
El Medano
Los Abrigos
$^{31}00$
Poris Formation exposure
towns
scoria cones
$^{3}30$
$^{3}40$
$^{3}50$

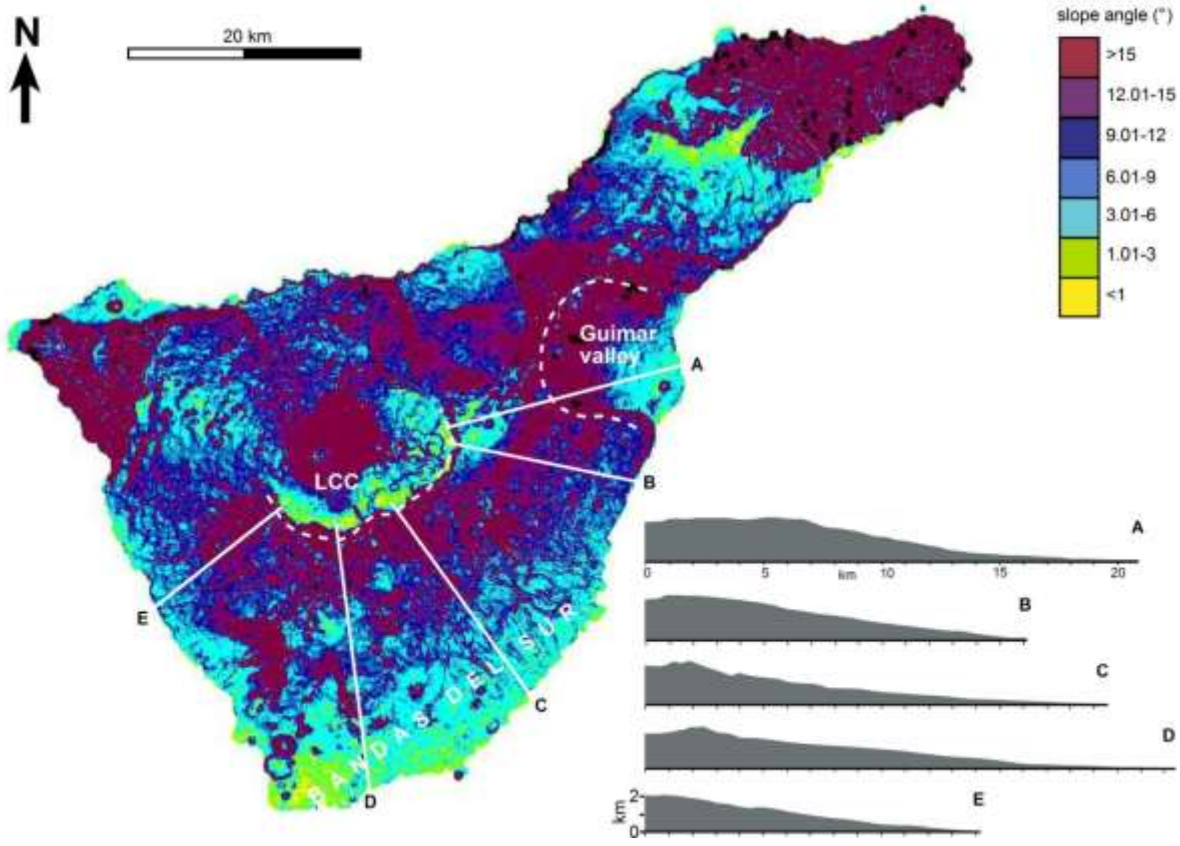

N
20 km
slope angle (°)
>15
12.01-15
9.01-12
6.01-9
3.01-6
1.01-3
<1
Guimar valley
LCC
BANDAS DEL SUR
A
B
C
D
E
0
5
km
10
15
20
km
2
0

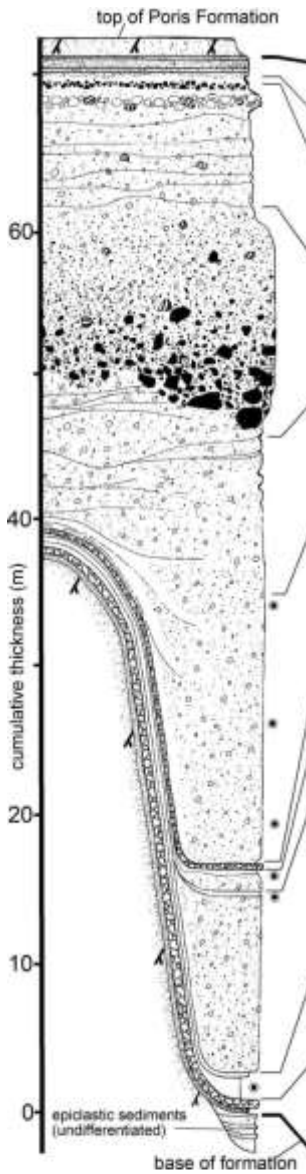

Member	Flow unit	Lithofacies	Lithology
11 (2 m) reworked Poris tephra			vitric sandstone; conglomerate lenses
10 (0.2 m) Plinian/sub-Plinian fall deposit	Flow-unit 4	mL	clast-supported banded pumice and lithic lapilli
9 (6 m) ignimbrite		mLT dbLT pLT	massive to diffuse-bedded lapilli-tuff
8 (15 m) ignimbrite		mLT dbLT lmBr ldbBr	massive to diffuse bedded lithic-rich lapilli-tuff with widespread lithic breccia layers; soft-sediment deformation of breccias common; thickens into depressions; first occurrence of banded pumice
7 (20 m) ignimbrite		mLT dbLT tsLT pLT xsLT	massive, stratified and diffuse-bedded lapilli-tuff; internal scours; intraclasts; lithic-breccia layers; overbank deposits <5 m thick; thickens to >20 m in palaeovalleys.
6 (20 m) ignimbrite		mLTacc dbTacc mTacc	valley-fill deposits comprise massive lapilli-tuff or tuff with scattered accretionary lapilli; rare lithic-rich layers; accretionary lapilli comprise ash/pumice/lithic cores with multiple concentric laminae; thins over topography into a thin diffuse-bedded tuff with abundant accretionary lapilli; occurs as a thin pellet layer in Guimar valley;
5 (0.2 m) Plinian fall deposit		mL	topography-draping pumice and lithic lapilli; drapes topography.
4 (0.9 m) ashfall and ignimbrite	Flow-unit 3	mTacc dbLT mLT	4B – framework--supported ash pellets; drapes topography; 2cm thick 4A – diffuse-bedded lapilli-tuff
3 (15 m) ashfall and ignimbrite	Flow-unit 2	mLT dbLT xsLT pLT mTacc dbTacc mTpel	3B - framework supported ash pellets; drapes topography; < 3 cm thick 3A – topography draping, bedded fine-grained tuff; scattered single-rimmed accretionary lapilli; loaded contacts; low-angle cross-stratification; thickens into depressions; valley-fill facies comprise massive, diffuse bedded and stratified lapilli-tuff; valley-margin deposits comprise massive fine-tuff and pumice-rich lapilli-tuff lenses.
2 (2.6 m) ashfall and ignimbrite	Flow-unit 1	mTacc mTpel	2B – framework supported ash pellets; drapes topography; gradational lower contact; <3 cm thick 2A – massive yellow vitric tuff with scattered accretionary lapilli; thickens into depressions; irregular, erosive lower contact
1 (1.3 m) Plinian pumice fall deposit		mL mT sT	Layer H: massive, well-sorted framework supported pumice lapilli deposit Layers A-G: stratified framework-supported pumice ash and lapilli, with minor lithic/obsidian clasts,

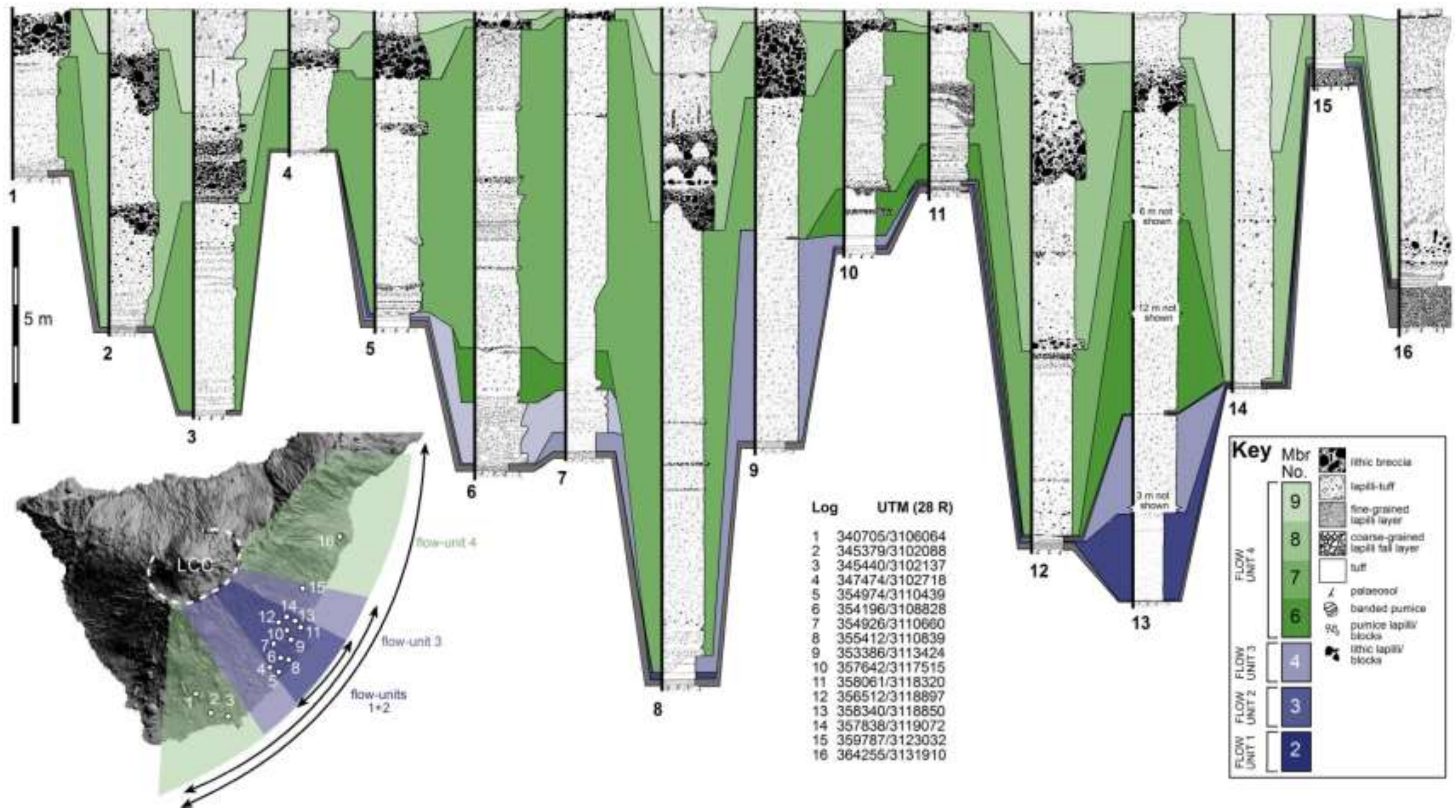
1
2
3
4
5
6
7
8
9
10
11
12
13
14
15
16
5 m
6 m not shown
12 m not shown
3 m not shown
LCC
flow-unit 4
flow-unit 3
flow-units 1+2
Log UTM (28 R)
1 340705/3106064
2 345379/3102088
3 345440/3102137
4 347474/3102718
5 354974/3110439
6 354196/3108828
7 354926/3110660
8 355412/3110839
9 353386/3113424
10 357642/3117515
11 358061/3118320
12 356512/3118897
13 358340/3118850
14 357838/3119072
15 359787/3123032
16 364255/3131910
Key
Mbr No.
FLOW UNIT 4
9
8
7
6
FLOW UNIT 3
4
FLOW UNIT 2
3
FLOW UNIT 1
2
lithic breccia
lapilli-tuff
fine-grained lapilli layer
coarse-grained lapilli fall layer
tuff
palaeosol
banded pumice
pumice lapilli/ blocks
lithic lapilli/ blocks

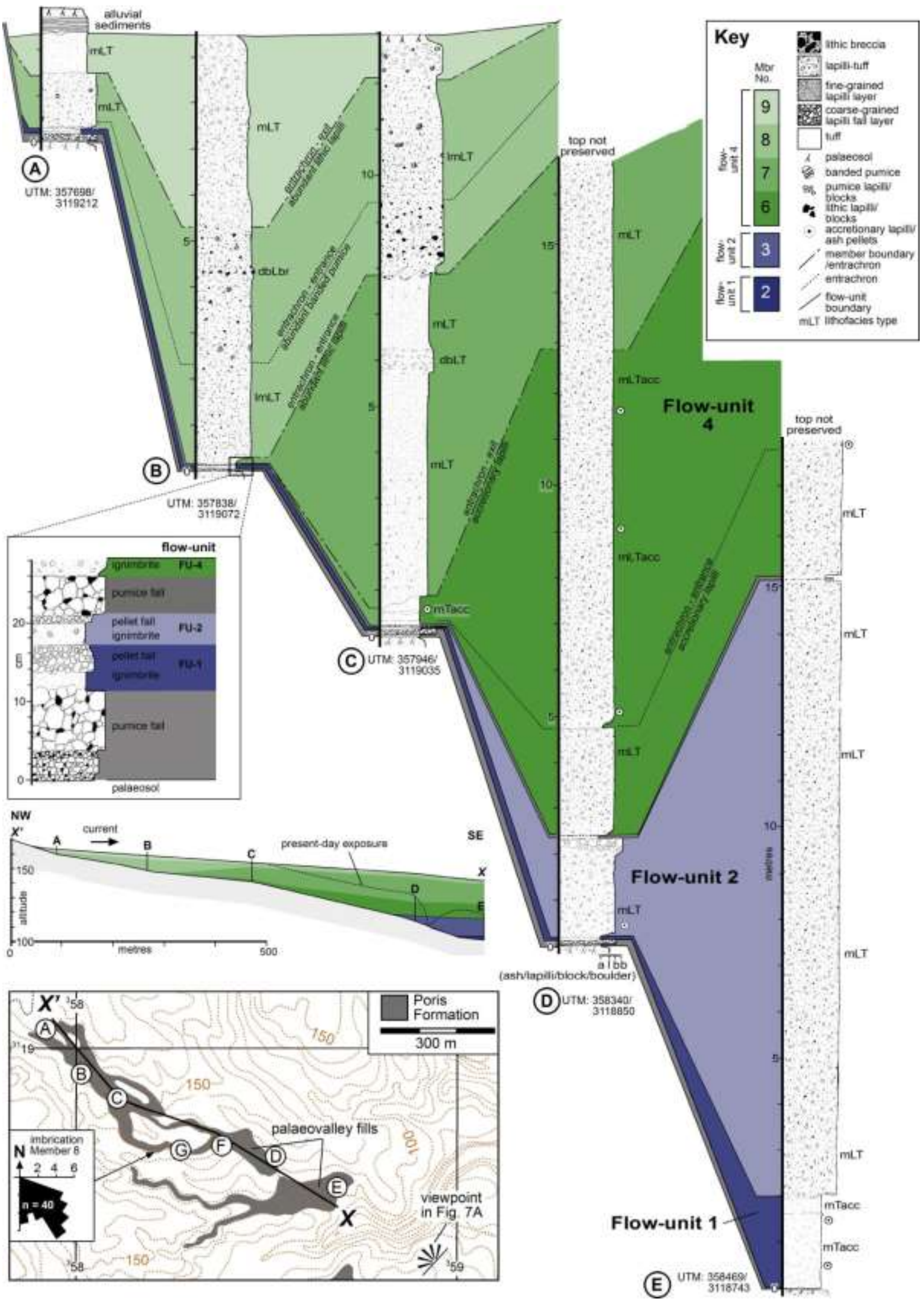

Key
lithic breccia
lapilli-tuff
fine-grained lapilli layer
coarse-grained lapilli fall layer
tuff
palaeosol
banded pumice
pumice lapilli/ blocks
lithic lapilli/ blocks
accretionary lapilli/ ash pellets
member boundary /entrachron
entrachron
flow-unit boundary
mLT lithofacies type
Mbr No.
flow-unit 4
flow-unit 2
flow-unit 1
alluvial sediments
UTM: 357698/ 3119212
UTM: 357838/ 3119072
UTM: 357946/ 3119035
UTM: 358340/ 3118850
UTM: 358469/ 3118743
top not preserved
Flow-unit 4
Flow-unit 2
Flow-unit 1
(ash/lapilli/block/boulder)
flow-unit
ignimbrite FU-4
pumice fall
pellet fall ignimbrite FU-2
pellet fall ignimbrite FU-1
palaeosol
NW
SE
current
present-day exposure
altitude
metres
Poris Formation
300 m
palaeovalley fills
imbrication Member 8
n = 40
viewpoint in Fig. 7A

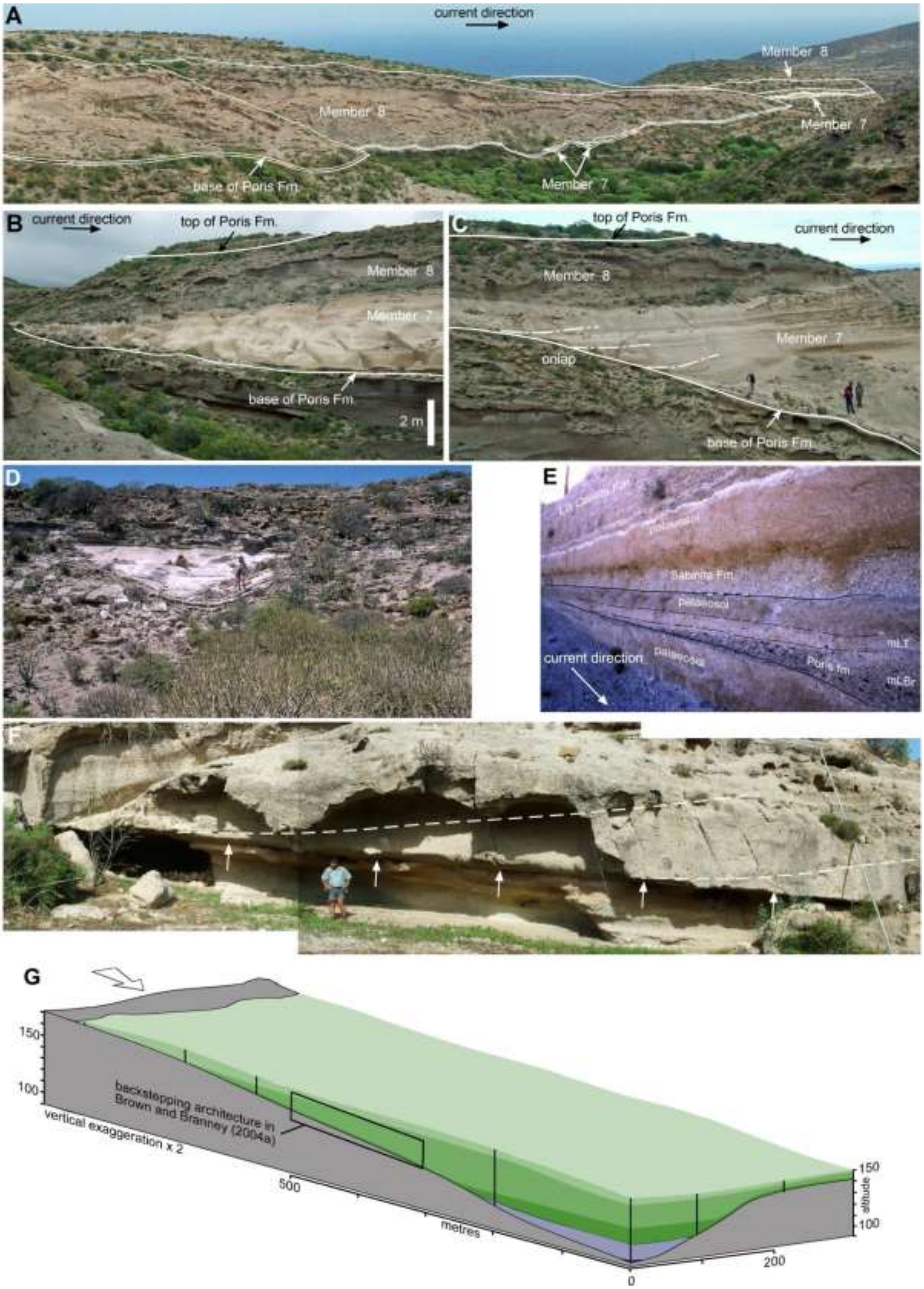
A
current direction
Member 8
Member 8
Member 7
base of Poris Fm.
Member 7
B
current direction
top of Poris Fm.
Member 8
Member 7
base of Poris Fm.
2 m
C
top of Poris Fm.
current direction
Member 8
Member 7
onlap
base of Poris Fm.
D
E
palaeosol
Sabinita Fm.
palaeosol
current direction
palaeosol
Poris fm.
mLT
mLBr
F
G
150
100
backstepping architecture in Brown and Branney (2004a)
vertical exaggeration x 2
500
metres
0
200
150
altitude
100

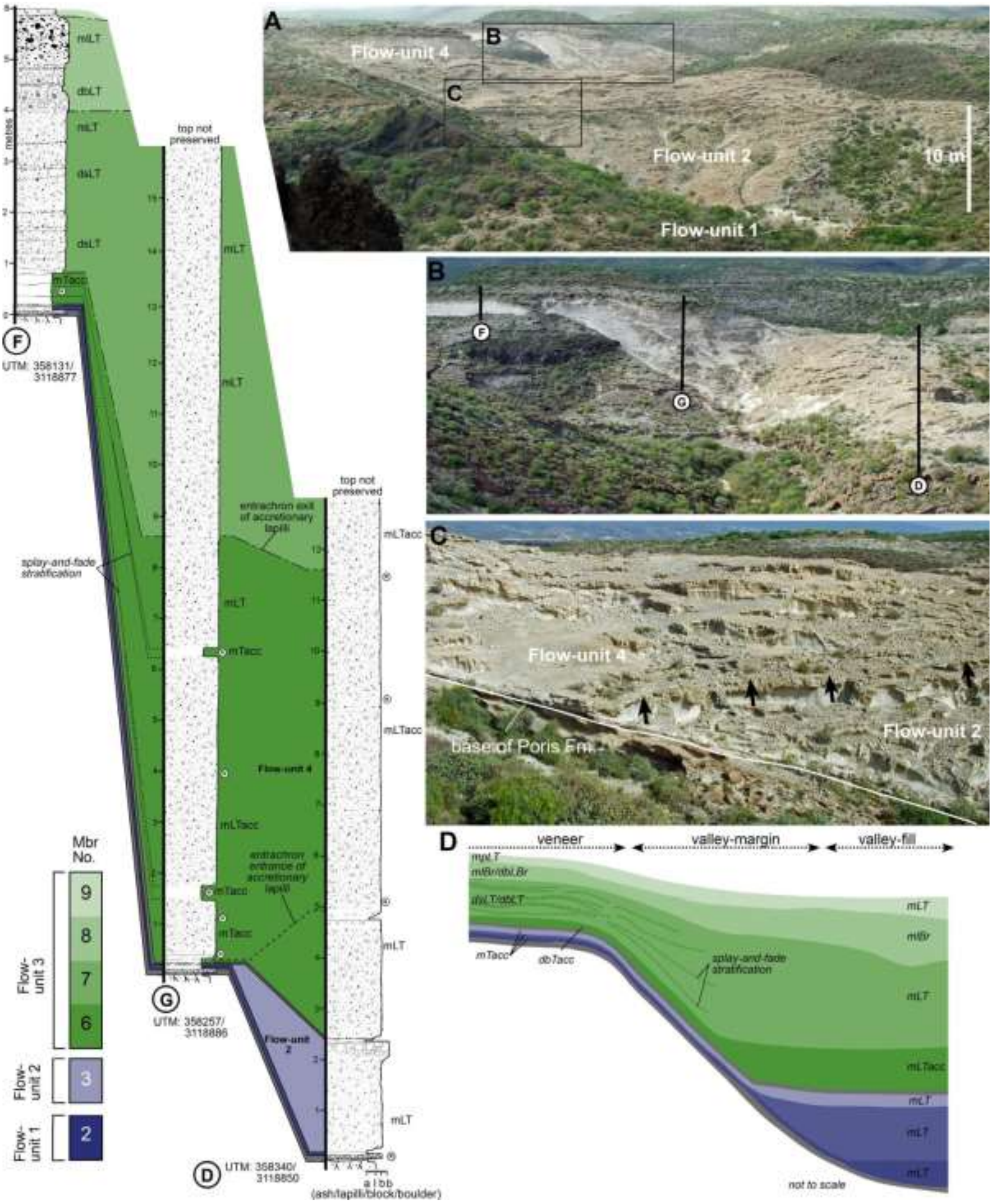

Flow-unit 4
Flow-unit 2
Flow-unit 1
10 m
base of Poris Fm.
veneer
valley-margin
valley-fill
splay-and-fade stratification
not to scale
top not preserved
entrachron exit of accretionary lapilli
entrachron entrance of accretionary lapilli
UTM: 358131/ 3118877
UTM: 358257/ 3118886
UTM: 358340/ 3118850
(ash/lapilli/block/boulder)
Mbr No.
Flow-unit 3
Flow-unit 2
Flow-unit 1


A
current
thin veneer ignimbrite
mantling lee side of cone
ignimbrite in B
B
Fasnia Formation ignimbrite
Plinian fall deposit
and thin ignimbrite
base of formation

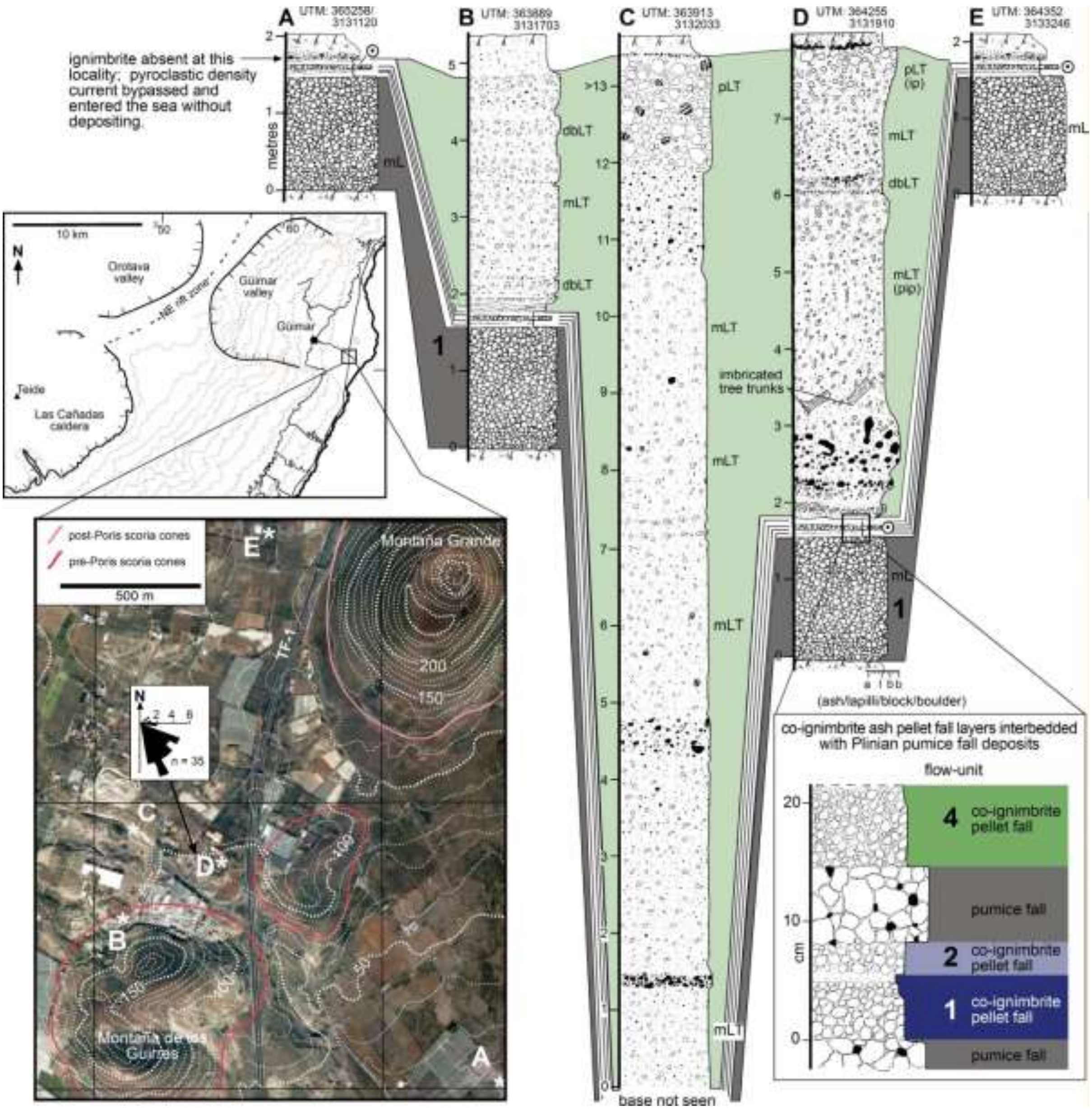

A UTM: 365258/ 3131120
B UTM: 363889 3131703
C UTM: 363913 3132033
D UTM: 364255 3131910
E UTM: 364352 3133246
ignimbrite absent at this locality; pyroclastic density current bypassed and entered the sea without depositing.
metres
mL
dbLT
mLT
pLT
pLT (ip)
mLT (pip)
imbricated tree trunks
base not seen
a l b bb
(ash/lapilli/block/boulder)
co-ignimbrite ash pellet fall layers interbedded with Plinian pumice fall deposits
flow-unit
4 co-ignimbrite pellet fall
pumice fall
2 co-ignimbrite pellet fall
1 co-ignimbrite pellet fall
pumice fall
cm
10 km
Orotava valley
Güimar valley
Güimar
NE rift zone
Teide
Las Cañadas caldera
post-Poris scoria cones
pre-Poris scoria cones
500 m
Montaña Grande
TF-1
n = 35
Montaña de las Guirres

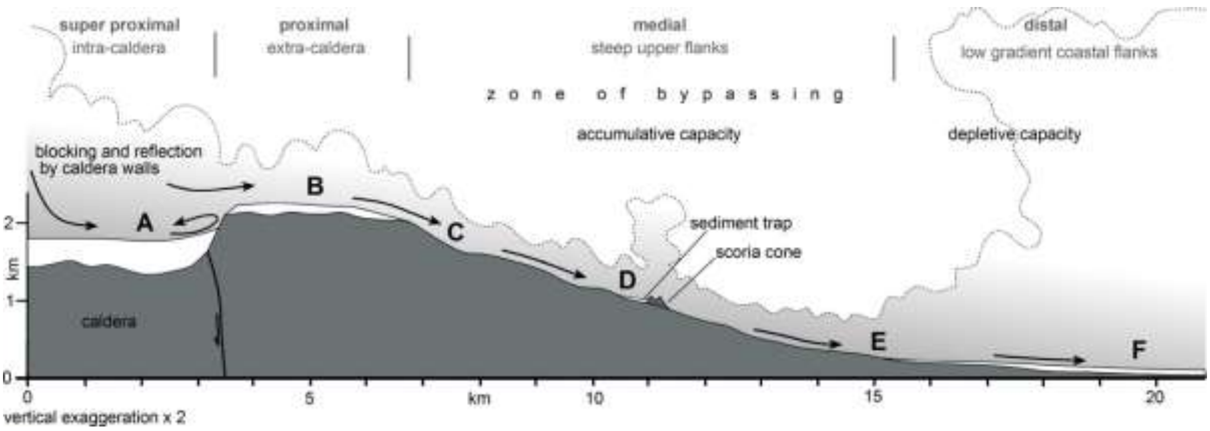

super proximal
intra-caldera
proximal
extra-caldera
medial
steep upper flanks
distal
low gradient coastal flanks
z o n e o f b y p a s s i n g
accumulative capacity
depletive capacity
blocking and reflection
by caldera walls
A
B
C
D
E
F
sediment trap
scoria cone
caldera
km
0
1
2
0
5
10
15
20
km
vertical exaggeration x 2

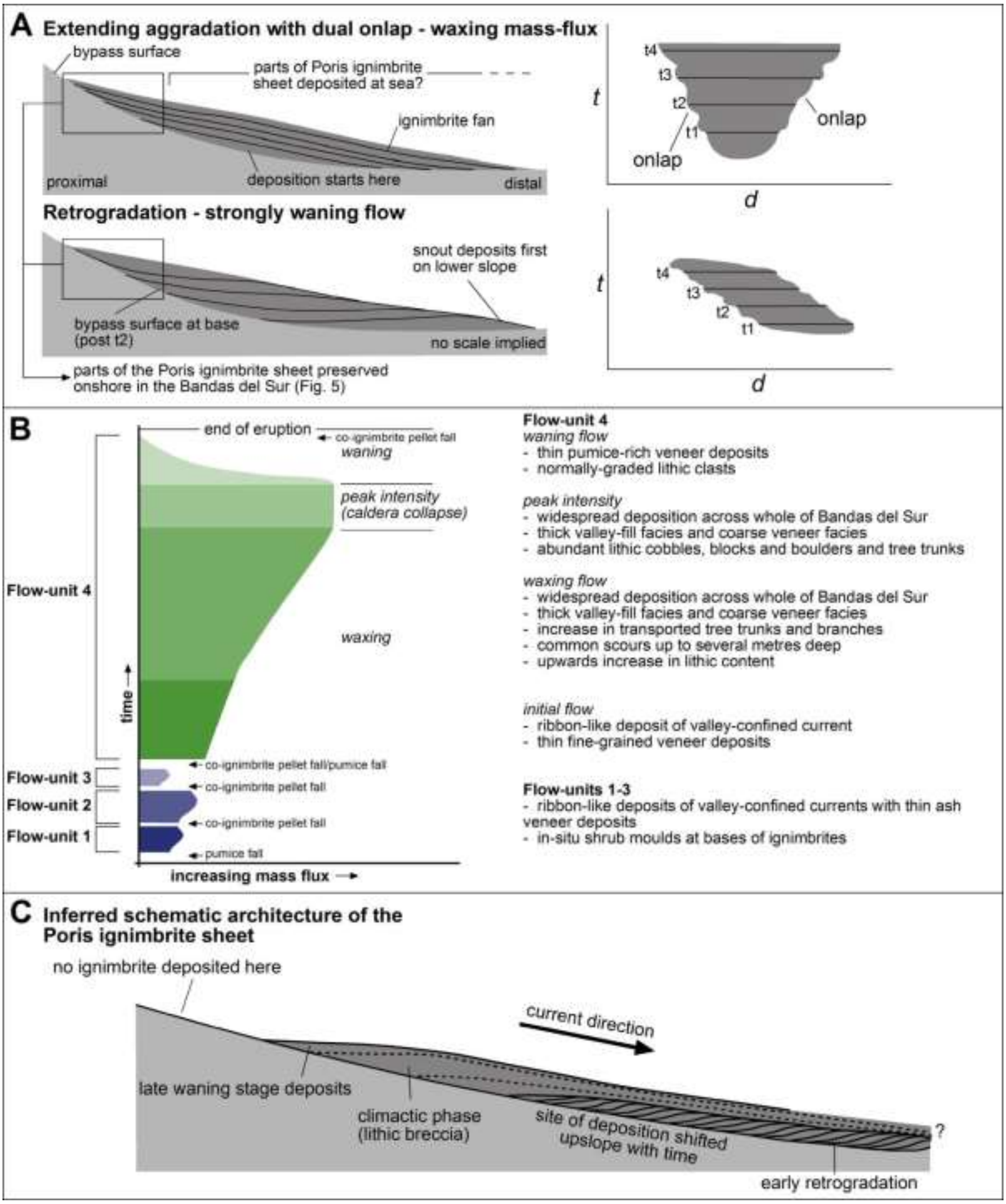
A Extending aggradation with dual onlap - waxing mass-flux
bypass surface
parts of Poris ignimbrite sheet deposited at sea?
ignimbrite fan
proximal
deposition starts here
distal
Retrogradation - strongly waning flow
snout deposits first on lower slope
bypass surface at base (post t2)
no scale implied
parts of the Poris ignimbrite sheet preserved onshore in the Bandas del Sur (Fig. 5)
t4
t3
t2
t1
t
onlap
onlap
d
t
d
B
end of eruption
co-ignimbrite pellet fall
waning
peak intensity (caldera collapse)
waxing
Flow-unit 4
time
co-ignimbrite pellet fall/pumice fall
co-ignimbrite pellet fall
co-ignimbrite pellet fall
pumice fall
Flow-unit 3
Flow-unit 2
Flow-unit 1
increasing mass flux
Flow-unit 4
waning flow
- thin pumice-rich veneer deposits
- normally-graded lithic clasts
peak intensity
- widespread deposition across whole of Bandas del Sur
- thick valley-fill facies and coarse veneer facies
- abundant lithic cobbles, blocks and boulders and tree trunks
waxing flow
- widespread deposition across whole of Bandas del Sur
- thick valley-fill facies and coarse veneer facies
- increase in transported tree trunks and branches
- common scours up to several metres deep
- upwards increase in lithic content
initial flow
- ribbon-like deposit of valley-confined current
- thin fine-grained veneer deposits
Flow-units 1-3
- ribbon-like deposits of valley-confined currents with thin ash veneer deposits
- in-situ shrub moulds at bases of ignimbrites
C Inferred schematic architecture of the Poris ignimbrite sheet
no ignimbrite deposited here
current direction
late waning stage deposits
climactic phase (lithic breccia)
site of deposition shifted upslope with time
?
early retrogradation